universität wien

MASTERARBEIT / MASTER THESIS

Titel der Masterarbeit / Title of the Master Thesis

"The influence of bilirubin on the uptake of 2-[^{18}F]fluoro-2-deoxy-D-glucose in C2C12 and HepG2 cells"

verfasst von / submitted by

Elisabeth Sperr, BSc

angestrebter akademischer Grad / in partial fulfillment of the requirements for the degree of

Master of Science (MSc)

Wien, 2018 / Vienna, 2018

Studienkennzahl lt. Studienblatt / degree programme code as it appears on the student record sheet:	A 066 838
Studienrichtung lt. Studienblatt / degree programme as it appears on the student record sheet:	Masterstudium Ernährungswissenschaften
Betreuer / Supervisor:	Univ.-Prof. Mag. Dr. Karl-Heinz Wagner

Acknowledgements:

I would like to express my big gratitude to Univ. Prof. Dr. Karl-Heinz Wagner for providing the possibility to do this interesting master thesis and for his great support and advice while supervising it. Another special thanks to Mag. Claudia Lang MSc for the discussions about the things I found out, about everything that didn't make sense to me and the always friendly advice.

A very dearly thanks to Mag. Eva-Maria Klebermass and Mag. Theresa Balber. Thank you for your constant support in planning and conducting my experiments from the first moment I got to your department and for making me feel welcome, encouraged and happy there.

I am also very thankful for the entire teams in the Department of Nutritional Sciences and the Department of Nuclear Medicine. My sincere thanks go to Yvonne Hirtl MSc and Antonia Klimpke BSc, for being not only my lab-partners but my companions throughout the whole project. Thank you for offering a helping hand whenever it was needed as well as for every joke we shared on long lab days. Without you it would have never been the same!

Many thanks go to my friends for supporting and motivating me throughout my study and this thesis. Thank you for the time you spent with me when I was barely able to talk about anything else but this project. For lending me an ear, some distraction or whatever I needed.

And finally, I would like to express my deep and infinite gratitude to my family. I am very thankful that you made this study possible for me and I feel blessed that you are there for me in all kinds of situations. Special thanks to my dad for constantly assisting me with useful ideas regarding this project and proofreading of this thesis.

Thank you!

Table of Contents:

List of Figures

List of Abbreviations

AMPK	adenosine monophosphate-activated protein kinase
ATCC	American Type Culture Collection
ATP	adenosine triphosphate
BLVRA	biliverdinreductase
B_{max}	number of receptors expressed on cells
BSA	bovine serum albumin
C2C12	skeletal muscle cell line C2C12
CPM	counts per minute
CPS	counts per second
CVD	cardiovascular disease
DIO (mice)	diet-induced obese (mice)
DMEM	Dulbecco's Modified Eagle's Medium
DMEM diff.	DMEM for differentiation
DMEM suppl.	DMEM supplemented
DMSO	dimethyl sulfoxide
^{18}F	fluorine-18
FBS	fetal bovine serum
[^{18}F]FDG	2-[^{18}F]fluoro-2-deoxy-D-glucose
FHS	fetal horse serum
GLUT	glucose transporter
GS	Gilbert's Syndrome
HepG2	hepatocarcinoma cell line HepG2
HO	heme oxygenase
IC_{50}	half maximum inhibitory constant (concentration of the radioligand causing 50% inhibition of radioligand binding)
K_d	equilibrium dissociation constant
K_i	equilibrium inhibitor constant
k_{on}	association rate constant
k_{off}	dissociation rate constant
LT	LigandTracer

MRP-2	multi-drug resistance protein-2
$NaHCO_3$	sodium bicarbonate
PBS	phosphate buffered saline
PET	positron emission tomography
P/S	penicillin, streptomycin
RCF	relative centrifugal force
RIA	radioimmunoassay
RL	radioligand
UCB	unconjugated bilirubin
UGT1A1	UDP-Glucuronosyltransferase 1A1

1. Introduction

Bilirubin is a bile pigment which occurs in the catabolism of heme. Following several catabolic steps, it is conjugated with a molecule of glucuronic acid for aqueous solubility, transported into the bile and excreted with the feces (1). In individuals with Gilbert's syndrome the step of glucuronidation is impaired and unconjugated bilirubin accumulates in the blood. In this benign metabolic disorder bilirubin levels of >17.1µM are observed, as compared to normal bilirubin levels of 3-17µM (2). The syndrome is associated with protection from cardiovascular disease (1), diabetes mellitus type 2 (3), inflammation and metabolic syndrome (4–6) as well as all-cause-mortality (7, 8). This is in contrast to other disorders including hepatitis, jaundice and cholestasis, where pathological, highly elevated levels of bilirubin are associated with the severity of the disease and thus with the amount of organ damage (9).

In this project we aimed at gaining a deeper understanding of the protective effects of mild hyperbilirubinemia. Therefore, we analyzed the influence of bilirubin on the uptake of glucose. We hypothesised that bilirubin increases the uptake of glucose. For this purpose, the uptake behaviour of the radioactively labelled glucose analogue, i.e. 2-[^{18}F]fluoro-2-deoxy-D-glucose ([^{18}F]FDG), was observed in murine muscle cells, i.e. C212 and human liver carcinoma cells, i.e. HepG2. Research was performed using conventional uptake assays in 6-well-plates and real-time uptake assays by LigandTracer® technology.

The project was conducted from December 2017 until May 2018 as a cooperation between the Department of Nutritional Sciences of the University of Vienna and the Division of Nuclear Medicine of the Medical University of Vienna.

2. Literature Review

2.1. Bilirubin

2.1.1. Structure and chemistry

Bilirubin is an orange to red coloured bile pigment which occurs in the catabolism of heme. It is a tetrapyrrolic, dicarboxylic acid which belongs to the family of porphyrins (10,11). Other tetrapyrrolic compounds include chlorophyll and bilins (e.g. phytochromobilin or phycocyanobilins). These pigments enable light-harvesting in higher plants, cyanobacteria and algae (11). There are two forms of bilirubin, first the form conjugated by glucuronic acids and second, the unconjugated form (9,11–14). Unconjugated bilirubin (UCB) consists of four pyrrolic rings which are linked by carbon bridges. The molecule is composed of two planar dipyrrole units and the structure is almost symmetrical. The dipyrroles consisting of two distinct monopyrroles, whereas they are connected by a saturated central methylene group (-CH2-). The interior monopyrroles have a carboxyethyl sidechain (-CH2-CH2-COOH) and the exterior ones contain a lactam group (-CO-NH-). An unsaturated methene group (-CH=) connects the two pyrrole rings within the dipyrrole units. Finally, the remaining sites on the pyrrole rings are occupied by an ethyl (-CH3) and a vinyl (-CH=CH2) group (11,12). These substituents are asymmetrically arranged and enable UCB's optical activity (11,12,15). The chemical structure is shown in Figure 1.

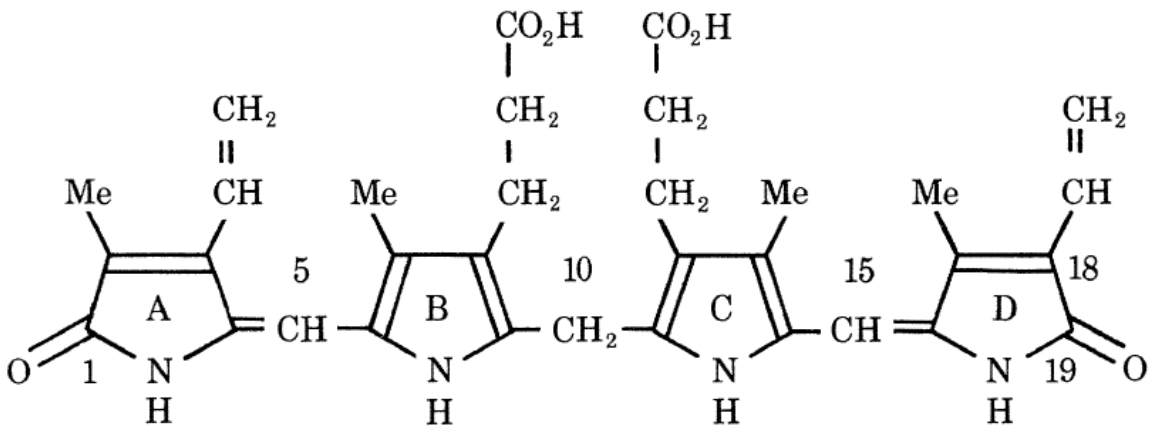

Figure 1: The tetrapyrrolic structure of bilirubin (10)

Despite the presence of several polar groups, bilirubin is poorly soluble in water (threshold of approximately 70nM (16,17)). The presence of internal hydrogen bonds existing between the propionic acid carboxyl- and the amino and lactam-groups accounts for this paradox, as shown in Figure 2 (10,11).

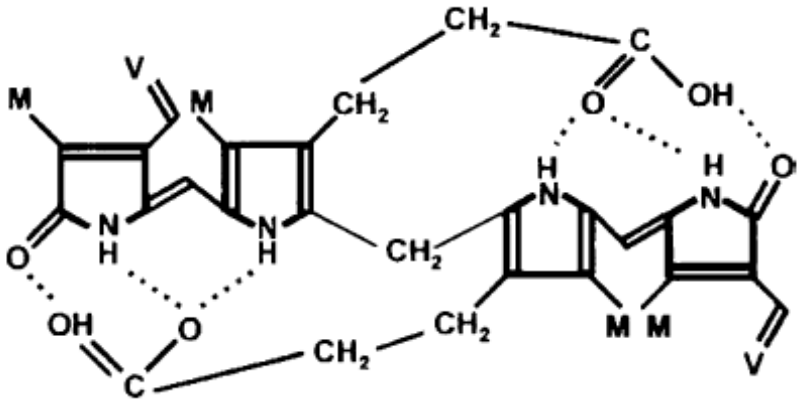

Figure 2: Internal hydrogen bonding within bilirubin (13)

2.1.2. Metabolism and physiology

Regarding the catabolism of heme, which uniquely occurs in mammals in this form, approximately 4mg/kg body weight of bilirubin are produced every day (1,13,14). Heme derives from hemoglobin which is released from senescent red blood cells and non-erythroid hemoproteins (18,19). Its catabolic pathway is of importance in the body's clearance of waste products (11). Within macrophages, in a first step heme is enzymatically converted to green biliverdin by heme oxygenase (HO) (as shown in figure 3). There are three known isoforms of HO. HO-1 is inducible by heme and oxidative stress and expressed predominantly in reticuloendothelial cells. HO-2 is non-inducible and constitutively expressed primarily in the central nervous system and testis. Finally, with a low catalytic activity HO-3 may function mainly as heme-binding protein (11,13). In this HO-dependent catabolic step, an iron molecule and one atom of carbon are liberated (1,9,13). The cytosolic biliverdin reductase (BLVRA) then reduces biliverdin to bilirubin by reduction of its central methine bridge (14). Due to UCB's poor aqueous solubility at physiological pH-value (16,17), it is solubilized by its binding to albumin and to apolipoprotein D in high density lipoprotein (11,12,20). In this form it is absorbed by hepatocytes and transported to the endoplasmatic reticulum. There, it undergoes glucuronidation by uridine glucuronosyl transferase 1A1 (UGT1A1) (21). This

facilitates excretion through the bile canaliculus in an ATP-dependent process by multi-drug resistance protein-2 (MRP-2) (1,11,13). In the gallbladder bilirubin glucuronides are stored and secreted into the gut to facilitate absorption of fat-soluble compounds. In this process bilirubin conjugates are deconjugated or reduced to urobilinogen which is mainly excreted in the stool, resulting in its distinct colour (9,13).

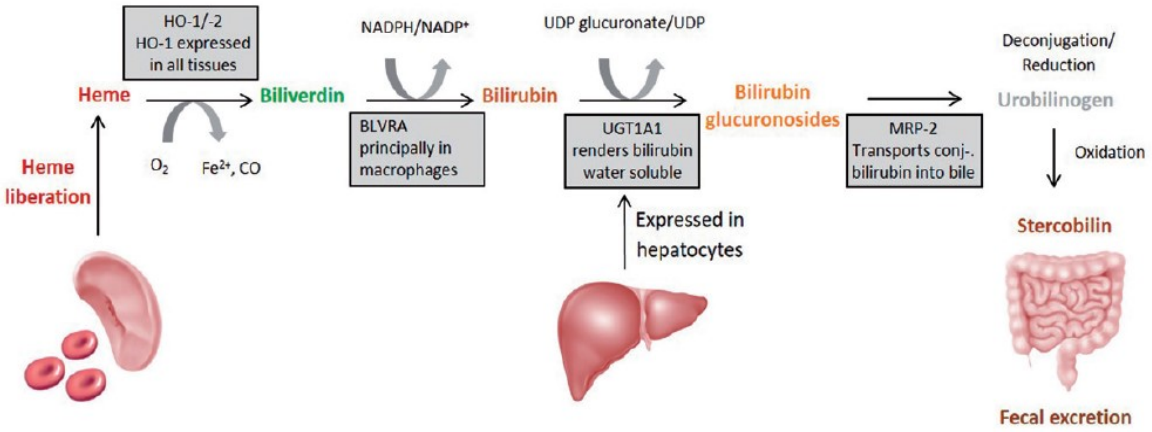

Figure 3: The catabolism of heme: Heme converts enzymatically to biliverdin and afterwards to bilirubin by reduction through BLVRA. Then, bilirubin is conjugated in the liver, requiring UGT1A1, and excreted into the bile by MRP2. Afterwards, the glucuronides are deconjugated again, forming urobilinogen which is mainly excreted fecally (9).

2.1.3. Toxicity and congenital conditions of impaired bilirubin excretion

The metabolic transformation and the excretion of bilirubin are of critical importance, since much higher plasma and tissue levels have cytotoxic properties (1,9,11). Hence, an accumulation of bilirubin can cause severe damage in the central nervous system. In daily clinical practice, bilirubin levels are measured to determine the cause of disease in patients with jaundice. In neonates for example, the intestinal flora is not fully capable of reducing UCB (22), contributing to neonatal jaundice. In addition, there is a number of other factors, including gender, hepatic stress and gastrointestinal transit time that influences this catabolic pathway and potentially leads to increased circulating bilirubin concentrations. An overview of these factors is provided in figure 4.

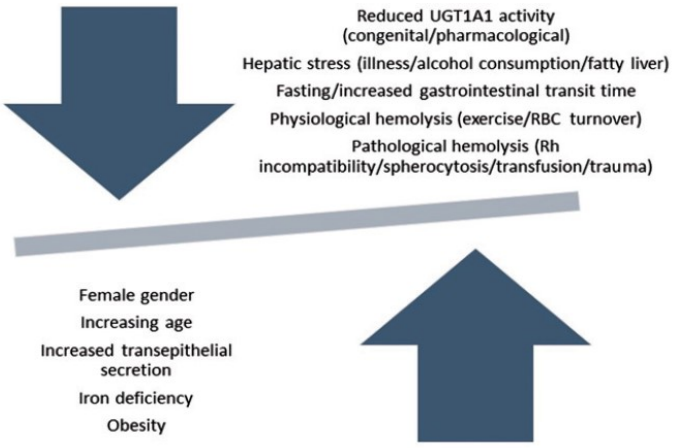

Figure 4: Factors increasing or decreasing the levels of serum bilirubin (9)

Several rare disorders of the bilirubin metabolism that require testing have been described including the Crigler-Najjar, Dubin-Johnson and Rotor syndrome. To differentiate between these disorders the knowledge of the cause of hyperbilirubinemia is of particular importance as demonstrated in figure 5 (9,23). A complete loss of UGT1A1 activity results in Crigler-Najjar syndrome type 1 (serum bilirubin levels 250-650µM), whereas a partial deficiency causes Crigler-Najjar syndrome type 2 (serum bilirubin levels 130-255µM) (23–25). Both syndromes are primarily diagnosed in early childhood soon after birth (9). Crigler-Najjar syndrome type 1 is associated with kernicterus. In these patients a life-long phototherapy (a process were bilirubin levels are reduced by the disruption of the hydrogen bonds within bilirubin by exposure to UV-light (13,15)) or in the case of severe hepatic dysfunction a liver transplantation is required (17,26). In contrast to Crigler-Najjar syndrome type 1, Crigler-Najjar syndrome type 2 is characterised by a milder course of the disease. Kernicterus only rarely appears and treatment with UGT1A1-inducing agents such as phenobarbitones is sufficient to stabilise the disease in most patients (27). A deficiency in MRP-2 results in the Dubin-Johnson syndrome. This shortage leads to an impaired transport of bilirubin. Thus the hallmarks of the disease are an accumulation of conjugated and unconjugated bilirubin in the plasma (9,13,17). This disorder has a benign course and does not require treatment (23). Similar laboratory findings are observed in patients with Rotor syndrome. Here, reduced hepatic storage capacity is responsible for the disorder (23,28). Like Dubin-Johnson syndrome, the Rotor syndrome is a benign condition which does not require specific treatment. Nevertheless, it is of importance to differentiate this disease from other hepatobiliary diseases (23).

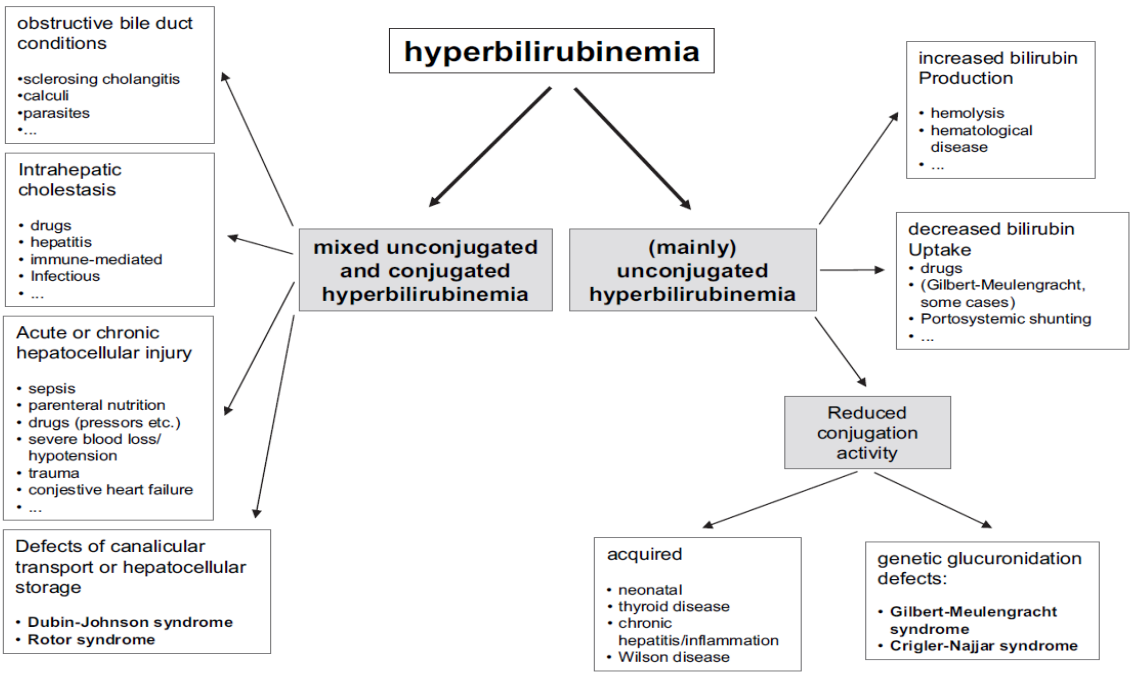

Figure 5: Effects of hyperbilirubinemia according to its origin (23)

2.2. Gilbert's syndrome

2.2.1. Definition

In contrast to Crigler-Najjar, Dubin-Johnson and Rotor syndrome, in cases with Gilbert's syndrome (GS) a mild elevation of UCB is found. This hereditary and chronic, yet benign syndrome was first described by Gilbert and Lereboulette in 1901 (29). It is found in up to 5% of the Caucasian, African and South Asian population (9,13). A lower prevalence of approximately 2% of GS is observed in individuals originating from Eastern Asia, whereas people with Indian or Middle Eastern ancestry show a GS prevalence of around 20% (9). In this metabolic disorder, the mechanism of UCB glucuronidation is impaired (~60%) by a common polymorphism in the UGT1A1 promoter region (UGT1A1*28 or UGT1A1*6). This polymorphism causes the insertion mutation of an additional TA residue in the TATA box (9,17,30). Thus, it leads to a decrease of approximately 70% in the expression of UGT1A1 and a diminished conjugation and excretion of bilirubin. Individuals with an increased number of TA repeats are often diagnosed with GS, which is defined by an unconjugated bilirubin concentration >17.1 µM. In general, circulating bilirubin concentrations in GS range from 17.1-85µM, and thus are markedly higher compared to normal bilirubin levels of 3-17µM (2,5,11,17,31). For the diagnosis of GS, blood is collected after an overnight fast and bilirubin

concentrations are examined. Individuals should demonstrate elevated bilirubin levels twice over a period of 6 months by having normal serum transaminases and markers of biliary damage (32). Jaundice is occasionally observed in GS when bilirubin concentrations exceed 40-45µM (9). This may occur in periods of stress, illness or fasting (33). Although GS individuals demonstrate higher bilirubin levels, the concentrations do not reach a level that causes neurological symptoms (9).

2.2.2. Potential beneficial effects of mild hyperbilirubinemia

Since the prevalence for non-communicable diseases increases all over the world, accurate biomarkers are needed for risk prediction. Bilirubin is suggested to be a promising marker in this aspect, since it shows interactions with several diseases (1). It is known that bilirubin has a strong antioxidative potential (34) and plasma UCB levels have been found to be directly correlated with serum and plasma antioxidant capacity (35). This antioxidant activity is of particular interest in case of cardiovascular disease (CVD). According to a theory, the oxidation of low density lipoprotein plays a central role in the pathogenesis of CVD. This process is inhibited by bilirubin (1). Indeed, Suh et al. reported a negative relationship between total bilirubin levels and incident coronary heart diseases and CVD deaths in a longitudinal study (36). Furthermore, mildly elevated concentrations of total bilirubin have been associated with health-promoting effects in diabetes mellitus type 2 (3,37), cancer mortality (38) and all-cause-mortality (7,8). Negative correlations were also found with inflammation and metabolic syndrome, suggesting an increased metabolic response in individuals with GS (4–6). However, considering the potential presence of many confounding variables the pronouncement of a cause-and-effect relationship is still under discussion (13). In this regard, such results should be handled carefully and further research is needed to determine the impact of mild hyperbilirubinemia in predicting and modulating disease processes (1).

2.3. Metabolism of glucose

Sugar, mainly glucose, is one of the most important sources of energy for cells. Therefore, glucose is stored as glycogen, with major depots located in muscle and liver tissue (39). For the absorption of polar molecules like glucose, these molecules need to cross semipermeable plasma membranes. This process is mediated by membrane-associated carrier proteins. There

are two families of carrier proteins, i.e. GLUT (solute carrier family 2; gene name: SLC2A) and SGLT (solute carrier family 5; gene name: SLC5A). GLUT transporters facilitate glucose translocation following existing concentration gradients, between external and internal sides of plasma membranes. In contrast, SGLT proteins are cotransporters for sodium and glucose. They transport glucose to the inside of cells against the gradient concentration. For this process energy is required constantly (40).

To transport glucose into liver cells, GLUT-2 is used, whereas GLUT-4 is important for the transport to skeletal muscle (41–43). After the absorption, the glucose molecules are used in (1) glycogen synthesis or (2) converted to pyruvate in glycolysis. In the first step of glycolysis, the enzyme hexokinase binds to the mitochondrial membrane and phosphorylates glucose to glucose-6-phosphate, which is a precursor for different glucose metaboliing pathways. During this process, glucose is catabolized to pyruvate and subsequently changed into acetyl-CoA, which is necessary in the mitochondrias' generation of ATP (44). In gluconeogenesis, glucose is build up when requirements exceed the availability of glucose. In liver and kidney cells the glucose-6-phosphate can therefore be reconverted to glucose. However, this is not possible in other mammalian tissues, due to a lack of glucose-6-phosphatase. Therefore and for hepatic utilisation and storage of glucose, the liver is a central point of glucose metabolism (45). Stored glycogen in muscle tissue is also used as energy resource since it is converted to glucose-6-phosphate if required, but this glucose-6-phosphate can be used for the cells' own requirements only (39).

In GS, blood glucose levels were found to be reduced. Mölzer et al. also observed that the activity of AMPK is increased in white blood cells of GS (5). This could suggest that the cellular uptake of glucose is enhanced in metabolically active cells. As a possible explanation an *in vitro* study by Cohen et al. shows that bilirubin increases the expression of GLUT-1 and the rate of glucose uptake (46). Hence, an increased metabolic response in individuals with GS is suggested, causing metabolic advantages regarding non-communicable diseases (4–6).

2.4. 2-[^{18}F]fluoro-2-deoxy-D-glucose – [^{18}F]FDG

2.4.1. Structure and chemistry

In this project, the uptake of glucose was examined by measuring the uptake of the radioactively labelled 2-[^{18}F]fluoro-2-deoxy-D-glucose ([^{18}F]FDG). The synthesis of non-

radioactive FDG was first described by Pacák, Točík and Černý from the Charles University in Prague in 1968 (47). Ten years later, in 1978, Ido and colleagues described the synthesis of FDG labelled with the radioisotope ^{18}F (48). Nowadays, 2-[^{18}F]FDG is a common radiopharmaceutical in medical imaging and the most widely used tracer in positron emission tomography (PET), due to its versatility (49,50).

Chemically, [^{18}F]FDG is a glucose analogue with a ^{18}F substitute for the hydroxyl group normally placed on C-2 of the glucose molecule (see Figure 6). ^{18}F decays with a half-life of 110 minutes, providing a sufficient signal for detection by using PET while keeping radiation burden for patients to a minimum (49).

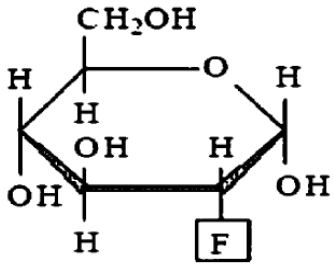

Figure 6: Chemical structure of 2-[^{18}F]fluoro-2-deoxy-D-glucose (modified from (49))

2.4.2. Radiosynthesis of [^{18}F]FDG

[^{18}F]FDG can be synthesised by two reactions, i.e. electrophilic fluorination and nucleophilic fluorination. The first synthesis was carried out using electrophilic fluorination (shown in Figure 7). [^{18}F]F_2 gas was added to the precursor 3,4,6-triacetylglucal across a double bond. This resulted in difluoride derivatives of the parent compound (3:1 ratio between difluoro-glucose and difluoro-mannose). In a final step, the difluoro-glucose derivatives were separated and hydrolysed by hydrochloric acid, yielding only 8% [^{18}F]FDG in 2 hours of synthesis (50,51).

Several improvements to electrophilic fluorination were made thereafter, but the major breakthrough was the development of the nucleophilic fluorination by Hamacher et al. in 1986 (52). In nucleophilic fluorination (shown in figure 8) a negatively charged nucleophilic molecule is added to a molecule with a leaving group. In the case of [^{18}F]FDG, mannose triflate is the precursor providing a leaving group with triflate at C-2 and [^{18}F]fluoride acts as the

nucleophile, substituting the leaving group and forming [^{18}F]FDG. Acetonitrile is used as solvent and Kryptofix 222^{TM} works as catalyst, increasing the reactivity of ^{18}F. This results in a yield of 50% with a shortened synthesis time of 50 minutes (50,52). Hence, nucleophilic fluorination was more widely used because of higher yield and shorter reaction time (49,50). Nowadays, the synthesis is performed in an automatic cassette-system. Within this system the process of synthesis takes 25 minutes and results in a yield of 70-80% (53).

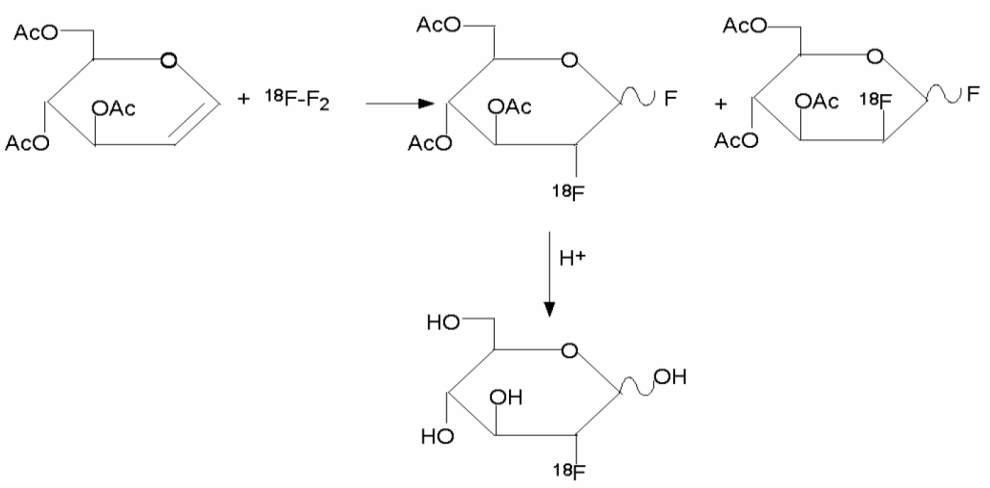

Figure 7: Synthesis of [^{18}F]FDG by electrophilic fluorination: Addition of fluorine atoms across the double bond of the precursor, resulting in difluoro derivatives and finally yielding [^{18}F]FDG after hydrolysis (modified from (50))

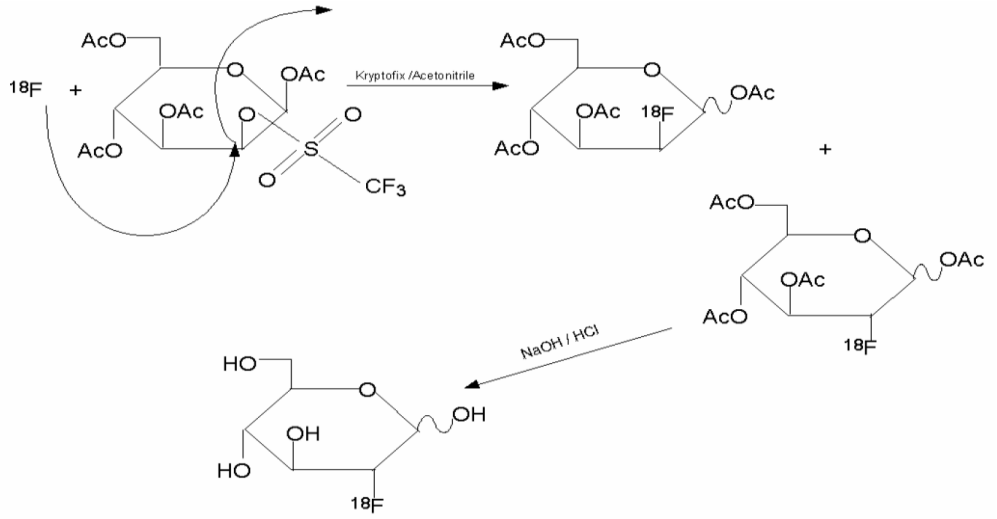

Figure 8: Synthesis of [^{18}F]FDG by nucleophilic fluorination: Substitution of the triflate leaving group and subsequent removal of the protecting groups yielding [^{18}F]FDG, catalysed by Kryptofix™. (modified from (50))

2.4.3. Metabolism of [^{18}F]FDG

[^{18}F]FDG is taken up by high-glucose-consuming cells, such as brain cells, brown adipocytes, kidney and cancer cells, similarly to glucose. Especially cancer cells are well known for their high metabolism resulting in an increased glucose uptake, caused by the Warburg effect (54,55). Hence, they incorporate higher amounts of [^{18}F]FDG than normal cells. Similar to glucose, the uptake of [^{18}F]FDG into living cells is facilitated by sugar transporters GLUT-1 to GLUT-5 (54,56). Especially GLUT-4 is used for the uptake into skeletal muscle (43), whereas GLUT-1 is the most important carrier in tumours (41,42). After the uptake, [^{18}F]FDG is enzymatically phosphorylated to FDG-6-phosphate by hexokinase. In contrast to glucose-6-phosphate, FDG-6-phosphate cannot be further metabolised in the glycolytic pathway, because the missing hydroxyl group on C-2 is mandatory for this step. Hence, it becomes metabolically trapped in the cell, although it can also be implemented into other pathways to be metabolised further (57,58). Nevertheless, this accumulation in cells and tissues over time is detectable by PET scanning facilities, forming two- or three-dimensional images of the distribution within the body (49). By this, [^{18}F]FDG is an appropriate surrogate for glucose uptake and cell viability (50,59,60).

2.5. Background of radioligand binding assays

Radioligand binding research is mainly used for the determination of ligand affinities to specific receptors and the analysis of the underlying mechanisms. Three different types of experiments can be differentiated, i.e. kinetic, saturation and competition assays (61,62).

The kinetic assays tend to be cumbersome and are mainly used to characterise novel radioligands (62). Furthermore, the establishment of optimal conditions for the experiment is of importance. The binding process of the radioactively labelled ligand is measured over time and thus information about association or dissociation from a particular receptor can be gathered. This information is represented by the association (k_{on}) and dissociation (k_{off}) rate constant (61).

Saturation and competition binding assays represent the group of equilibrium studies (61,62). The underlying theory is that the association of the ligand with its receptor and the

dissociation of the ligand-receptor complex are reversible processes (62). Both occur until a state of equilibrium is reached. Incubation time, temperature during incubation and assay volume are of importance in the development of equilibrium conditions (62). In saturation binding studies the affinity of a radioligand for a receptor is examined (62,63). Several concentrations of a radioactively labelled ligand are used to test its affinity to the receptor and are measured at this equilibrium (61). In saturation assays the concentration where the radioligand occupies 50% of available receptors is determined. This represents the equilibrium dissociation constant (K_d), a measure for the affinity of the radioactively labelled ligand to the receptor. Hence, the affinity to the receptor is higher when only a low concentration is needed (62). The calculation of K_d is shown in Figure 9. In addition, the number of receptors expressed on cells is determined, representing the maximal binding capacity of the receptors (B_{max}) (63).

$$K_d = \frac{k_{off}}{k_{on}} = \frac{[\text{ligand}] \times [\text{receptor}]}{[\text{receptor} \cdot \text{ligand}]}$$

Figure 9: Calculation of the equilibrium dissociation constant K_d by using association (k_{on}) and dissociation (k_{off}) rate constant (61)

However, in competition binding studies the characterisation of the receptor is determined by inhibition of radioligand binding (62). Experiments are performed by using only one single concentration of the ligand but several concentrations of a competing, not radioactively labelled substance (61–64). Here, the concentration of the competitive inhibitor causing 50% inhibition of binding (IC_{50}) is examined (62,63). Instead of the equilibrium dissociation constant K_d, the equilibrium inhibition constant for binding of the unlabelled drug (K_i) is used to express the affinity (65). K_i is calculated by using the Cheng-Prusoff equation as shown in figure 10.

$$K_i = \frac{IC_{50}}{1 + \frac{[RL]}{K_d}}$$

Figure 10: Calculation of the equilibrium inhibition constant K_i by using the concentration of the competitive inhibitor causing 50% inhibition of binding (IC_{50}), the concentration of the used radioligand (RL) and the equilibrium dissociation constant (K_d) (65)

2.6. Real-time assays using LigandTracer® technology

The technology of LigandTracer® (LT) was first described by Björke and Andersson at the University of Uppsala in 2006 (66). Today, the technology can be purchased from Ridgeview Instruments AB (Uppsala, Sweden) and is frequently used in research (67,68). The method provides a semi-automated monitoring of the interactions between ligands and adherent cells in real-time. Therefore a rotating radioimmunoassay (RIA) principle is used (69). Not only information about the affinity of the ligand, but also about kinetics of cell uptake or retention can be received (66,69).

To conduct an experiment with LT, cells are seeded only on one half of the circular culture dish (i.e. ~4cm² area near the edge of the dish), denoted the target area. The opposite half without any cells is designated as the reference area, the so-called "background" (69). The culture dish is placed on a tilted support in the device and measured for the required period. During the measurement, the dish is continuously rotated on this inclined support. This enables the detector above to screen either target or background (69–71). As shown in figure 11, the radioactively labelled solution accumulates at the bottom of the dish. Thus, it is not in the field of detection, although the thin remaining fluid film can be measured in both areas (66). The output signal represents the difference between the maximum radioactivity of the target and the lowest radioactivity of the background (69).

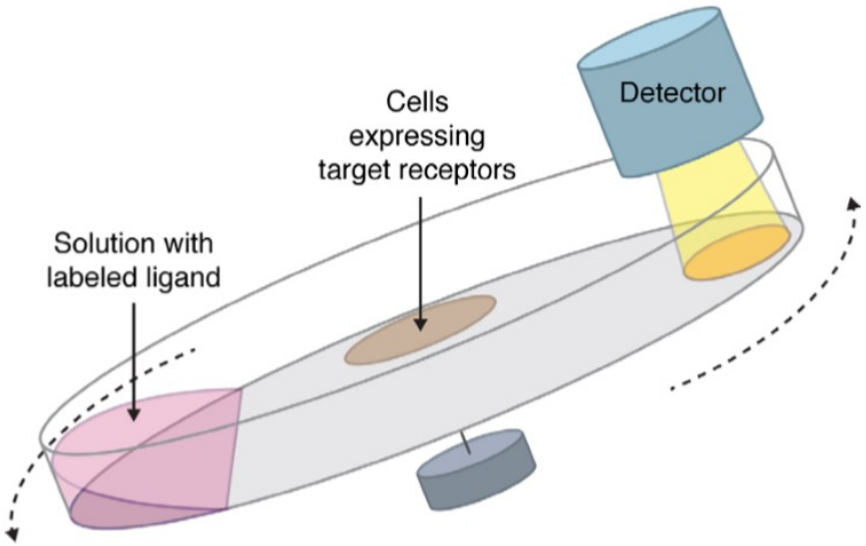

Figure 11: Schematic representation of LigandTracer® technology (71)

The output signal reflects the amount of cell-associated radioligand, providing an accurate estimation of the kinetics of the interaction over time (70–72). The signals, per rotation round in counts per second (CPS), are put together forming a curve which exhibits the amount of ligand interacting with a receptor or – in the case of [^{18}F]FDG – the amount of a drug taken up during the measurement (see figure 12).

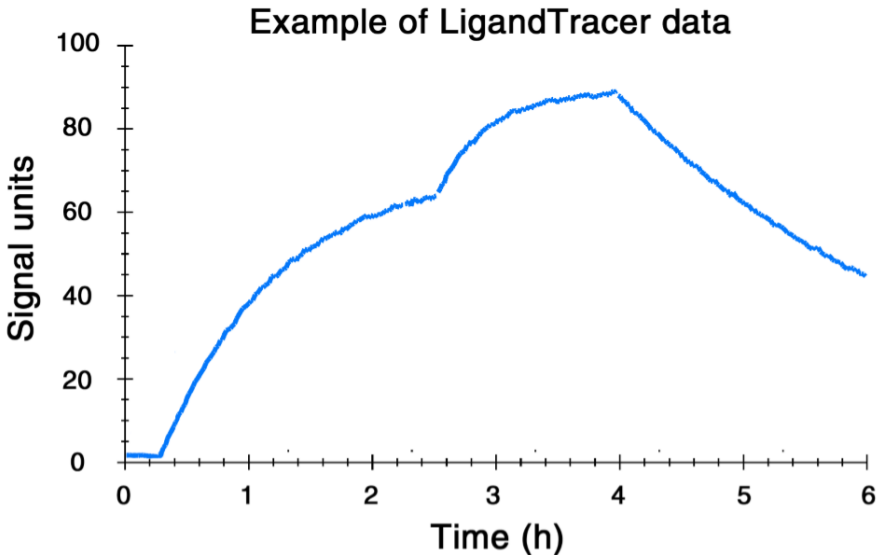

Figure 12: Example of a kinetic binding curve, obtained from LigandTracer® technology (70)

There are a few important advantages within this technology for kinetic measurements. First, the semi-automated device is very sensitive, simple in terms of handling and saves time as well as reagents (66,69). Thus, it improves productivity in comparison to manual methods. In addition, it addresses environmental as well as safety issues relating to the use of radioactive isotopes (66). Second, the uptake over time is visualised and can therefore be evaluated by the high-resolution binding trace (69,71). Third, the interactions between ligand and cells can be followed in real-time (69). Forth, an in situ reference area is used for background correction and makes the measurement insensitive for background or reagent-mediated radiation (66). Fifth, the device is able to work at room temperature, as well as in cold rooms or in the incubator (72). However, also some disadvantages must be considered. The first disadvantage is that cells need to be adherent to stand the continuous rotation. Thus, cells in suspension cannot be used, unless they are previously anchored to the dish surface (69). Moreover, the current technology does not allow leaving the lid on the dish, which makes vaporisation a serious problem if the measurement chamber is not properly sealed (69). Lastly, for our

specific experimental setting only dishes from the same day are comparable. Hence, experiments with short-lived radionuclides or long incubation times demand access to more than one device from the same type (i.e. LT yellow, LT green, LT grey and LT white), because it is not possible to parallelise measurements within one instrument at present (69).

2.7. Cells

Two cell lines were used for the research in this project. The muscle cell line C2C12 and the hepatic cancer cell line HepG2. Both cell lines were purchased from American Type Culture Collection (ATCC, Manassas, Virginia, USA) and kindly provided by the Department of Nutritional Sciences and the Department of Pharmacognosy of the University Vienna.

The cell line C2C12 (ATCC CRL-1772) is an immortalised subclone of the murine myoblast cell line established by Yaffe and Saxel at the Weizman Institute of Science in Israel in 1977 (73,74). These myoblasts are adherent and have a doubling time of 12 hours. The C2C12 cell line differentiates after a supplementation with horse serum, forming contractile, polynuclear myotubes and producing characteristic muscular proteins (75). Physiologically, glucose uptake by a variety of peripheral tissues including skeletal muscles is important in the maintenance of glucose homeostasis (76). Thus, the evaluation of bilirubin induced effects in these cells was of particular interest in this project.

As a second cell line, HepG2 was chosen. Originally, these nowadays immortalised cells derived from a hepatocellular carcinoma tissue of a 15 year old Caucasian boy (77). They have a lot of cellular functions similar to normal hepatocytes. Therefore, they are a proper model for in vitro research (78–80). Hence, among various hepatocellular carcinoma cell lines, HepG2 is one of the most extensively used in research. In our project the use of liver derived cells was necessary because of their involvement in the hepatic utilisation, storage and production of glucose (45).

3. Material & Methods

3.1. Materials & Equipment

3.1.1. List of materials

- **Accutase solution:** for cell culture, sterile filtered, Sigma-Aldrich, product-code: A6964
- **Bilirubin:** powder, >98%, Sigma-Aldrich, product-code: B412
- **Bovine Serum Albumine:** BSA, Sigma-Aldrich, Fraction V Fatty Acid Free Roche 10775835001
- **C2C12 cells**: ATCC CRL-1772
- **Dimethyl sulfoxide:** DMSO, Sigma-Aldrich, product-code: D8418
- **Dulbecco's Phosphate Buffered Saline:** PBS, for cell culture, liquid, sterile filtered, modified without calcium chloride and magnesium chloride, Sigma-Aldrich, product-code: D8537
- **Dulbecco's Phosphate Buffered Saline:** PBS, for cell culture, liquid, sterile filtered, modified without calcium chloride and magnesium chloride, Gibco, product-code: 14190
- **Dulbecco's Modified Eagel's Medium:** DMEM, for cell culture, liquid, sterile filtered, with 4500mg/L glucose and sodium bicarbonate, without L-glutamine, sodium pyruvate and phenol red, Sigma-Aldrich, product-code: D1145
- **Dulbecco's Modified Eagel's Medium:** DMEM, for cell culture, liquid, sterile filtered, without glucose, L-glutamine and phenol red, Gibco, product-code: A1443001
- **Dulbecco's Modified Eagel's Medium powder:** DMEM powder, for cell culture, powder, without glucose, L-glutamine, sodium bicarbonate and sodium pyruvate, Sigma-Aldrich, product-code: D5030
- **2-[^{18}F]fluoro-2-deoxy-D-glucose:** [^{18}F]FDG, produced at the Division of Nuclear Medicine, Medical University of Vienna, Vienna General Hospital.
- **Fetal Bovine Serum:** FBS, for cell culture, liquid, sterile filtered, Gibco, product-code: 10270
- **Fetal Horse Serum:** FHS, for cell culture, liquid, sterile filtered, Gibco, product-code: 10500-056
- **Glucose:** D-Glucose, Sigma-Aldrich, product-code: D8270

- **HepG2 cells:** ATCC HB-8065
- **Hydrochloric acid:** HCl, 25%, Sigma-Aldrich, product-code: 30723
- **L-Glutamine:** for cell culture, liquid, sterile filtered, BioXtra, 200mM, Sigma-Aldrich, product-code: G7513
- **Linoleic acid sodium salt:** >98% (GC), Sigma-Aldrich, product-code: L8134
- **Sodium hydroxide:** NaOH, pellets, Sigma-Aldrich, product-code: 06203
- **Sodium oleate:** ≥99%, Sigma-Aldrich, product-code: O7501
- **Sodium palmitate:** ≥98.5%, Sigma-Aldrich, product-code: P9767
- **Penicillin-Streptomycin:** P/S, for cell culture, liquid, sterile filtered, 10.000 units penicillin and 10mg streptomycin per millilitre in 0.9% sodium chloride, BioReagent, Sigma-Aldrich, product-code: P0781
- **Trypan blue:** 0.4% for application for cell counting with automated cell counter, Life Technologies, product-code: T10282

3.1.2. List of equipment

- **6-well-plates:** VWR, Tissue Culture plates 6 wells, sterile, product-code: 734-2323
- **6-well-plates AKH:** Techno Plastic Products AG, Tissue Culture Testplate 6, product-code: 92406
- **Aspiration System:** Vacuumbrand, Diaphragm vacuum pump, serial no. 18265907-94
- **Aspiration System AKH:** Integra Vacusafe + Integra Vacuboy
- **Cell Counter:** Luna Dual Fluorescence Cell Counter
- **Cell Counting Slides:** Luna Cell Counting Slides
- **Cell Culture Flasks:** 75cm² Cellstar Cell Culture Flasks
- **Cell Scepter AKH:** Millipore Scepter 2.0 Handheld Automated Cell Counter
- **Cell Scepter Tips:** Millipore Scepter Cell Counter Sensors 40µM
- **Cell Scepter Tips:** Millipore Scepter Cell Counter Sensors 60µM
- **Centrifuge:** Eppendorf Centrifuge 5417 R
- **Centrifuge:** Heraeus Megafuge 1.0 R Centrifuge
- **Centrifuge AKH:** Hettich Lab Technology Rotanta 460RC
- **Dishes:** Cellstar Cell Culture Dishes 100x20mm
- **Eppi Tubes:** Biozym Scientific GmbH, reaction vessel, 1.5mL amber

- **Eppi Tubes:** Semadeni AG, FlipTube, 1.5mL transparent
- **Eppi Tubes AKH:** Eppendorf Safe-Lock Tubes 1.5mL transparent, mix
- **Eppi Tubes AKH:** Eppendorf Safe-Lock Tubes 2mL transparent, mix
- **Eppi Tubes AKH:** Eppendorf Safe-Lock Tubes 5mL transparent, mix
- **Gamma Counter:** Perkin Elmer, 2480 Wizard^2 Automatic Gamma Counter
- **Graduated Pipette AKH:** VWR Disposable Serological Pipets 5mL, sterile
- **Graduated Pipette AKH:** VWR Disposable Serological Pipets 10mL, sterile
- **Graduated Pipette AKH:** VWR Disposable Serological Pipets 25mL, sterile
- **Incubator:** Heraeus Instrument, Function Line BB16
- **Incubator AKH:** Heraeus Heracell 150
- **Incubator AKH:** Labotect Inkubator C200
- **Laminar flow cabinet:** Bioair Safemate 1.8
- **Laminar flow cabinet AKH:** Kojair BioWizard Silver SL-130
- **LigandTracer:** Ridgeview Instruments, LigandTracer® Yellow
- **Magnetic stirrer:** Heidolph MR 3001 K
- **Microscope:** Hund Wetzlar Wilovert S
- **Microscope AKH:** Olympus CK2
- **Pasteur Pipettes:** 250, No. 567/2, 230mm, Assistent
- **Pasteur Pipettes AKH:** VWR, product-code: 747720 ab250L
- **pH meter:** Metrohm 827 pH lab
- **Pipette:** 0.5-5mL Eppendorf Research plus
- **Pipette:** 100-1000µL Eppendorf Research plus
- **Pipette:** 20-200µL Eppendorf Research plus
- **Pipette:** 10-100µL Eppendorf Research plus
- **Pipette:** 2-20µL Eppendorf Research plus
- **Pipette:** 0.5-10µL Eppendorf Research plus
- **Pipet Controller:** AccuPet AccuHelp Motorized Pipette Controller
- **Pipet Controller AKH:** Integra Pipetboy acu 2
- **Scale:** Mettler Toledo XSE 205 Dual Range
- **Test Tubes:** 15mL brown, VWR Centrifuge Tube
- **Test Tubes:** 15mL transparent, Cellstar Centrifuge Tube

- **Test Tubes:** 50mL transparent, Cellstar Centrifuge Tube
- **Vortex:** Heidolph Reax 2000
- **Vortex AKH:** VELP Scientifica 2x³
- **Waterbath:** Gesellschaft für Labortechnik GFL1002
- **Waterbath AKH:** Thermo Scientific TSGP05

3.2. Cell Culture

3.2.1. Cultivation of C2C12 cells

The mouse muscle myoblast cell line C2C12 was kept and cultured at the laboratories of the Department of Nutritional Sciences of the University Vienna. Cells were grown in supplemented Dulbecco's Modified Eagel's Medium (DMEM suppl.) i.e. Dulbecco's Modified Eagel's Medium supplemented with 10% fetal bovine serum (FBS), 2% L-glutamine and 1% penicillin/streptomycine (P/S). The myoblasts were passaged two times a week when a confluence of 70-80% was reached. It must be noted that it is of critical importance that cultures are not allowed to become fully confluent because the cells can begin to fuse and partially differentiate upon cell to cell contact (see Figure 13) (74). Thus, sticking to a strict routine is important when working with this cell line. Proliferation took 3, respectively 4 days at a temperature of 37°C and a CO_2 content of 5%.

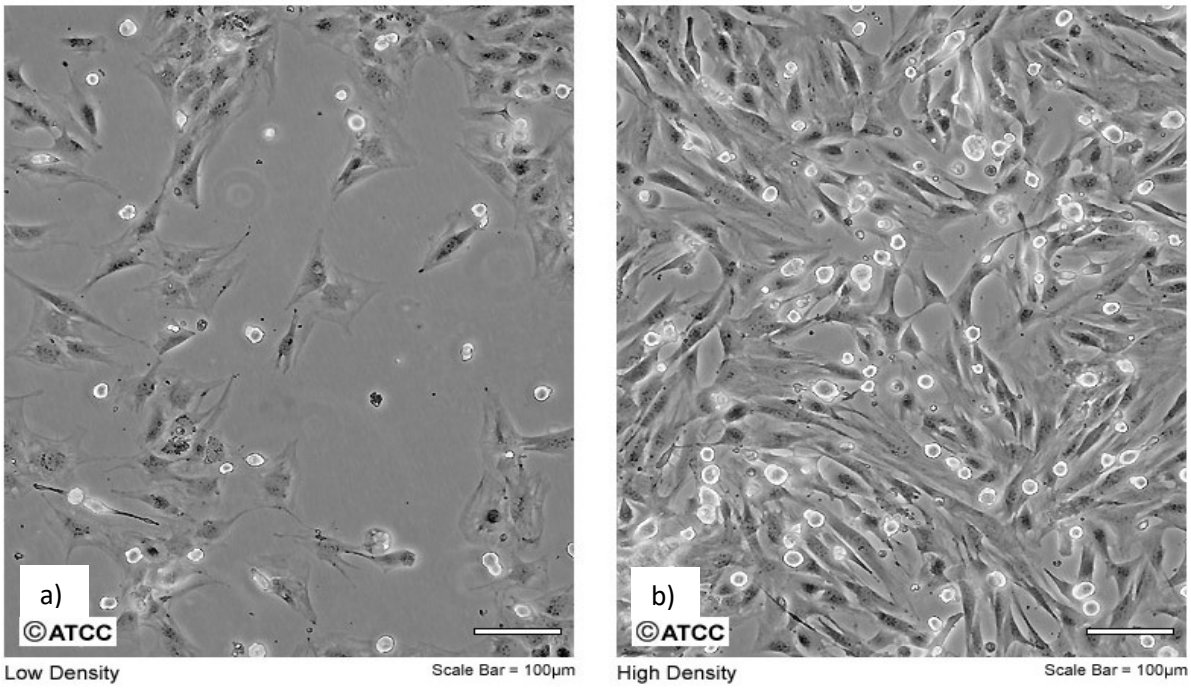

Figure 13: Phase contrast micrographs of C2C12: a) myoblasts at low confluence after 1 day of

proliferation and b) myoblasts at high confluence after 3 days of proliferation. The spindle-shaped appearance of the cells can be observed (modified from (74))

For passaging, cells were first gently washed once with phosphate-buffered saline (PBS) (37°C) after the old medium had been removed. This is important in order to rinse off the remaining proteins from the medium. Then the cells were detached from the flask surface by incubation with 3mL of the proteolytic enzyme Accutase for 5 minutes at 37°C. The activity of the enzyme was stopped by adding 6mL of DMEM suppl. The detached cells were transferred from the flask to a 15mL centrifuge tube and centrifuged for 5 minutes at 20°C at 179g. Thereafter, the pellet of cells was resolved in PBS and the number of cells/mL was calculated with the Luna Dual Fluorescence Cell Counter. After another centrifugation for 5 minutes at 20°C with a RCF of 179g the cells were resolved in DMEM suppl. $0.3x10^6$ or $0.2x10^6$ cells in 10mL DMEM were seeded into cell culture flasks with a surface of $75cm^2$ for 3 or 4 days of proliferation respectively.

3.2.2. Freezing and unfreezing of C2C12 cells

For freezing, cell passaging was performed as usual. After the second centrifugation however, the cell pellet was dissolved in a freezing medium instead of DMEM. The freezing medium was composed of 90% FBS and 10% dimethyl sulfoxide (DMSO). Cells were frozen in 1.8mL of the freezing medium at a density of $3.6x10^6$ and kept at a temperature of -80°C for 24 hours to allow freezing of -1°C per hour. The cryotubes were then stored in liquid nitrogen at the temperature of -196°C.

For thawing the cells, a cryotube was taken from the tank with liquid nitrogen and rehashed quickly. As soon as it was partially thawed, it was transferred and dissolved in 8mL of warmed DMEM suppl. (37°C). Then the cells were centrifuged for 5 minutes at 20°C with a RCF of 179g. It is of importance that those steps are performed rapidly, since the DMSO in the freezing media is cytotoxic and could damage cells (81). Finally, the cells were resolved in 12mL DMEM suppl. and seeded into 3-4 $75cm^2$ flasks. The flasks were incubated at a temperature of 37°C and a CO_2 content of 5%, until a confluence of at least 60% was reached and routine passaging could be started.

3.2.3. Routine of HepG2 cell cultivation

The cell line HepG2 was kept and cultured at the laboratories of the Division of Nuclear Medicine of the Medical University Vienna. The medium for this cell line consisted of DMEM, 10% FBS (for HepG2 a different FBS was used than in cultivation of C2C12), 2% L-glutamine and 1% P/S (DMEM suppl.). The protocol for cell cultivation was similar to the routine of the C2C12 myoblasts. Likewise, the proliferation took 3, respectively 4 days at a temperature of 37°C and a CO_2 content of 5%. Passaging of HepG2 cells was performed at a confluence of 80-95%. In contrast to the C2C12 cells, HepG2 do not differentiate and confluence is not critical. Nonetheless, a standardised cultivation pattern is of importance to ensure an accurate base for the experiments (see figure 14). Passaging was performed two times a week with a seeding density of $5.0x10^6$ and $4.3x10^6$ cells per 25mL DMEM suppl. for 4 and 3 days respectively in cell culture flasks with a surface of $175cm^2$.

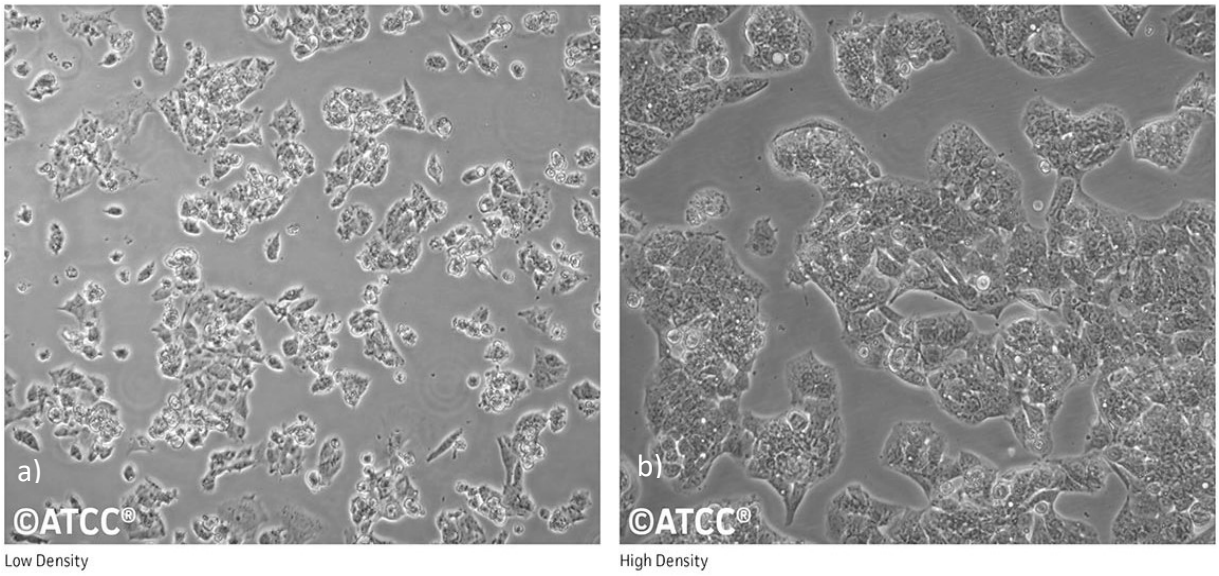

Figure 14: Phase contrast micrographs of HepG2: a) cells at low confluence after 1 day of proliferation and b) cells at high confluence after 3 days of proliferation. The spherical shape of the cells can be observed. (modified from (77))

The protocol for passaging the HepG2 cells was analogue to the protocol of C2C12 cells except from the volume of Accutase (7mL), the following incubation time (6 minutes) and the device for cell counting (Millipore Scepter 2.0 Handheld Automated Cell Counter).

3.2.4. Preparation of the stocks and treatments

For the experiments a vehicle control containing bovine serum albumin (BSA) and DMSO was prepared. The UCB treatments contained BSA, DMSO and 17.1µM and 55µM UCB. 3 stocks were prepared as vehicle control and bilirubin treatment prior the experiments, i.e. the BSA-stock (0.4545mM BSA), and DMSO-stock (0.825% DMSO in 0.4545mM BSA) as vehicle control and the BR stock (0.165mM UCB in 0.4545mM BSA). Since the uptake of glucose was of particular interest, each of the stocks was prepared with and without addition of glucose (+Glu treatment: 4.5g glucose/1 L of sterile filtered water; -Glu treatment: no glucose).

The first preparation step of each stock was to dissolve BSA powder in sterile filtered water. To enhance the solution process, a magnetic stirrer was used stirring continuously and keeping the solution at a temperature of 37°C for 20 minutes. The solution of BSA in water was supplemented with 4mM L-glutamine, a solution of DMEM (0.83g DMEM powder/100mL sterile filtered water) and a solution of sodium bicarbonate (0.37g $NaHCO_3$/100mL sterile filtered water). If glucose was needed in the stock, it was added to a final concentration of 450mg/dL. This was the BSA stock. To prepare the remaining 2 stocks, DMSO or UCB was added to the BSA-stock.

Since UCB is insoluble in water it was dissolved in DMSO at a concentration of 20mM. The solution was vortexed for 10 seconds, kept at 70°C in a water bath for 5 minutes and vortexed 10 seconds for the second time. Then it was sonicated for 1 minute and vortexed 10 seconds for the third time. Finally, a centrifugation at 4°C for 30 seconds with a RCF of 14,000g was conducted. If crystals were present, the procedure had to be repeated. To bind UCB to the BSA-stock, the pH-value of the stock was adjusted to an alkaline value >7.7 at a temperature of 37°C. Moreover, after the addition of the UCB-DMSO-solution to the BSA-stock, the tube was shaken vigorously for 30 seconds and afterwards gently in the water bath for 5 minutes at 37°C. Finally, the stock was again examined for crystal formation under the microscope. In case of the presence of yellow to orange crystals in the stock, a new stock had to be prepared. Since UCB is light-sensitive, it is important to work with UV-opaque materials and a minimum of lighting during the whole process (11).

The DMSO stock was prepared analogously to the UCB-stock. Instead of 20mM UCB-DMSO, DMSO was added to the BSA-stock and the solution was analyzed for crystallization products.

Finally, the pH of all stocks was adjusted to 7.36-7.44, representing the physiological conditions in the blood. To store them properly they were finally filtered sterile, aliquoted and frozen at -20°C for a maximum of 3-4 months.

3.3. [^{18}F]FDG Uptake with 6-well-plate assay

3.3.1. Protocol of [^{18}F]FDG Uptake with 6-well-plate assay

For the quantitative evaluation of the effects of bilirubin on the glucose uptake of C2C12 and HepG2 cells, the uptake of [^{18}F]FDG in these cells was measured with the gamma counter. In these experiments 0.16x10^{6} C2C12 cells and 1.2x10^{6} HepG2 cells per well were seeded in 6-well plates in 4mL or 2mL of DMEM suppl. respectively. A confluence of 100% was reached after 2 days of proliferation. Subsequently, the proliferation medium in the dishes was exchanged for the differentiation medium, DMEM diff. This consisted of Dulbecco's Modified Eagel's Medium (DMEM), 10% horse serum (FHS), 2% L-glutamine and 1% penicillin/streptomycine (P/S). It took the myoblasts from day 3 to day 9 to differentiate and experiments were conducted with the formed myotubes (Figure 15). Therefore, the myotubes were exposed to treatment and vehicle control for [^{18}F]FDG uptake experiments. This stimulation of differentiation was not necessary in HepG2 cells. In these cells the [^{18}F]FDG uptake experiments were performed on day 3.

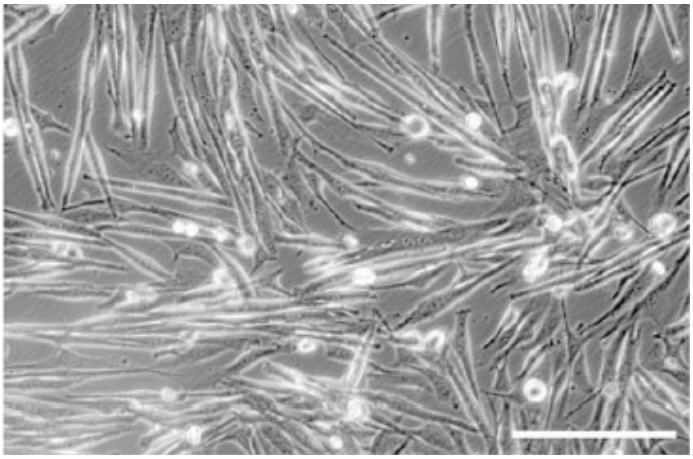

Figure 15: C2C12 myotubes after 6 days of differentiation (modified from (82))

For the [^{18}F]FDG uptake the cells were incubated with treatment containing 17.1µM or 55µM UCB, analogously to physiological conditions, or vehicle control (450mg/dL glucose). They were incubated for 5 and 24 hours respectively, followed by 2 hours of starving without glucose, but in presence of UCB. This starvation is important for achieving a sufficient radioactive signal. In each 6-well-plate 3 wells were used for the vehicle control and the other 3 for the treatment with bilirubin, as shown in figure 16. In brief, after the incubation with +Glu and -Glu, 150 kBq of [^{18}F]FDG were added to each well, followed by an incubation for 60 minutes at 37°C. In addition, three eppi tubes with 1.5mL PBS were treated with [^{18}F]FDG at the same time. This was done in order to monitor the radioactive decay as a 100% reference.

After the incubation with [^{18}F]FDG the radioactively enriched supernatant was removed from each well and collected in 5mL eppi tubes. Then, the cells were washed twice with 1mL of PBS. Each washing fraction was added to the supernatant of the respective well. Afterwards, the cells were detached by using 0.5mL of Accutase for 5 minutes in case of C2C12 and 7 minutes in HepG2, as described previously. The activity of the enzyme was stopped by adding 1mL of PBS to each well. The cells were re-suspended and transferred to 2mL eppi tubes, before they were counted by the Millipore Scepter 2.0 Handheld Automated Cell Counter. Finally, the vials with references, supernatants and cell fractions were measured in 2480 Wizard² Automatic Gamma Counter for 30 seconds.

3.3.2. Data analysis of gamma counter outcome

The results were obtained as counts per minute (CPM). For data management these results were transferred into an Excel file. In a first step, the relative uptake of [^{18}F]FDG was calculated in percentage of vehicle control, to adjust for variances between different days of experiments. Afterwards, descriptive statistics, i.e. mean, standard deviation and standard error of the mean, were determined. For further analysis, GraphPad Prism (GraphPad Prism 6, GraphPad Software, San Diego, USA) was used. To evaluate whether differences between treatment and vehicle control were of statistical significance, the unpaired t-test was used after testing on normality. A p-value <0.05 was considered significant. Values are expressed from at least three individual experiments performed in triplicates.

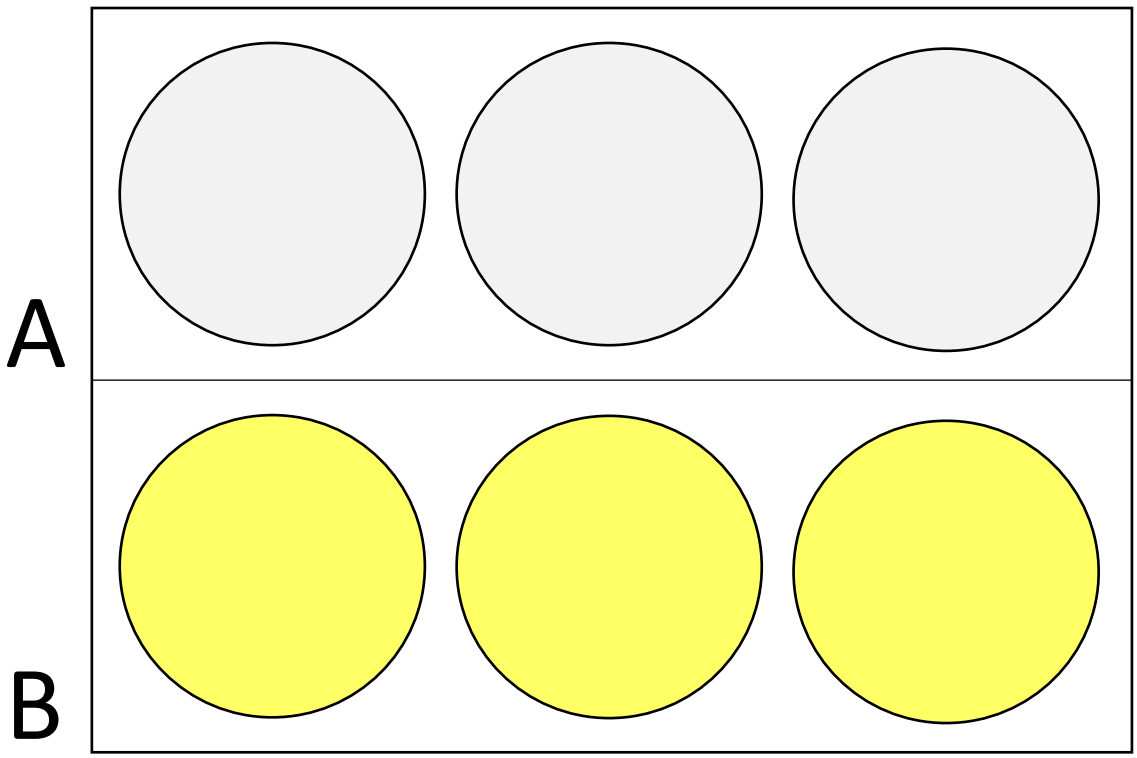

Figure 16: Experimental setup in 6-well-plates for the FDG-uptake with the gamma counter. In the upper line A, the cells were treated with vehicle control (i.e. BSA stock + DMSO stock) and in the bottom line B, UCB treatment was applied at different concentrations (i.e. 17.1µM and 55µM UCB)

3.4. [^{18}F]FDG Uptake using LigandTracer® Yellow

3.4.1. Protocol of [^{18}F]FDG Uptake using LigandTracer® Yellow

Regarding the usage of the C2C12 cells in our LT experiments, the [^{18}F]FDG uptake was performed in cell culture dishes with a surface of 20cm^2. Therefore 0,8x10^6 cells were seeded with 4mL of DMEM suppl. In order to achieve cell growth only on one half of the dish, since the opposite side should be used as a reference, the dish was placed in the incubator in an inclined angle. After proliferation for 2 days, a confluence of 100% was reached. To induce differentiation in C2C12 cells they were incubated with 6mL of DMEM diff. for 6 days. Thereafter, the myotubes were exposed to treatment and vehicle control for [^{18}F]FDG uptake experiments.

The [^{18}F]FDG uptake LT experiments using HepG2 were done according to the same protocol as with C2C12. In brief, 8.0x10^6 HepG2 cells were seeded in the dishes with 4mL of DMEM

suppl. and the proliferation took 3 days. As differentiation cannot be induced in this cell line, no differentiation medium was needed, and the experiments were conducted on the 4th day at a confluence of 100%.

For the experiments with LT technology, it was of importance that only dishes of the same day were comparable. Prior to the treatment, cells were washed with 4mL of PBS. In an experiment, a dish with vehicle control was compared to dishes with 17.1µM or 55µM UCB in cell line C2C12. For experiments with HepG2 concentrations with 17.1µM or 55µM UCB were used likewise. The cells were treated with 4mL of treatment and incubated at 37°C for different durations. Similar to the well-plate assay, cells were first treated with UCB for 5 and 24 hours and then starved for 2 hours in the presence of UCB.

To generate an accurate baseline, the LT had to be started without culture dish or added radioactivity at least 10 minutes prior measurement. The calculated volume for 150 kBq of [^{18}F]FDG was added to the dish and the uptake was measured for 60 minutes. The whole procedure was repeated with the following dishes.

3.4.2 Data analysis of LigandTracer® outcomes

The curves obtained from the experiments were used to analyze the relative tracer uptake in treatment samples compared to vehicle control, i.e. qualitative evaluation. They were not further subjected to quantitative analysis. The curves were processed by TraceDrawer™ (Ridgeview Instruments AB, Uppsala, Sweden). To enable a proper comparison between vehicle control and treatment, overlays of curves generated on the same day were created using this software.

4. Results

4.1. [^{18}F]FDG Uptake with 6-well-plate assay

To evaluate whether bilirubin influences the uptake of glucose in tissues we performed a 6-well-plate assay. In this assay the effects of UCB on C2C12 and HepG2 cells regarding the uptake of [^{18}F]FDG and the clearance of [^{18}F]FDG in the supernatant were observed. Since the influence of bilirubin is assumed to be very small and cells are susceptible biological systems, this clearance of the supernatant was also important for ensuring reproducibility. Concentrations and incubation time was chosen based on previous experiments, where effects of bilirubin on lipid cell metabolism and lipid uptake were observed after 5 hours of bilirubin incubation (unpublished data). Thus, experiments were started with an incubation time of 5 hours. To assess a potential time-dependency, the incubation time was prolonged to 24 hours to provide a greater challenge. Furthermore, to examine the dose-dependency of bilirubin, experiments were started with a concentration of 17.1µM UCB, the lower cut-off level for GS. Subsequently, the concentration was increased to 55µM UCB.

All 6-well-plate assay experiments were performed in triplicates, three times each. Since the influence of bilirubin was of main interest, the results show the accumulation of [^{18}F]FDG per 1x10^{5} cells and are presented as comparison of the bilirubin treatment to the vehicle treatment in % of vehicle.

4.1.1. Treatment with glucose

4.1.1.1. 5 hours +Glu in C2C12

To examine the potential cellular changes induced by UCB, cells were treated with UCB for 5 hours. Glucose-containing treatment (+Glu) was chosen to ensure optimal conditions for cells during treatment with UCB. [^{18}F]FDG was evaluated after 2 hours starving without glucose (-Glu). In the cellular fraction of C2C12 this setting resulted in an increased [^{18}F]FDG uptake. These differences were of statistical significance (Figure 17A, $p=0.03$). However, there was no significant decrease of [^{18}F]FDG in the supernatant (Figure 17B, $p>0.05$).

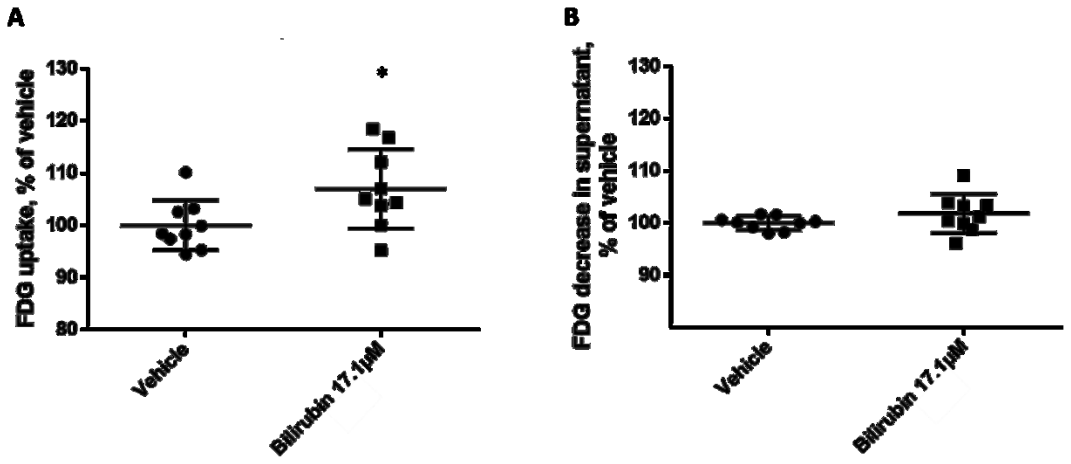

Figure 17: Uptake of [^{18}F]FDG in cellular fractions and decrease of [^{18}F]FDG in the supernatant after treatment with +Glu for 5 hours and -Glu for 2 hours in C2C12: A) results after treatment with 17.1µM UCB in cellular fractions (p=0.03) and B) results after treatment with 17.1µM UCB in the supernatant (p=0.19)

4.1.1.2. 5 hours +Glu in HepG2

The same experimental settings were repeated with HepG2. In this cell line, the uptake of [^{18}F]FDG in the cellular fraction was elevated following incubation with UCB at 17.1µM or 55µM. With regard to the statistical testing, the incubation with 17.1µM UCB resulted in a trend, but no significance was proved (Figure 18A, p=0.09). This strong tendency was not found analysing the differences observed at 55µM (Figure 18C, p>0.05). The increased [^{18}F]FDG uptake in the cellular fraction resulted in a decrease of [^{18}F]FDG in the supernatant which was observed at both concentrations, 17.1µM UCB and 55µM UCB. However, the difference between vehicle and UCB-treatment were only statistically significant following 17.1µM UCB (Figure 18B, p=0.02) but not after treatment with 55µM UCB (Figure 18D, p>0.05).

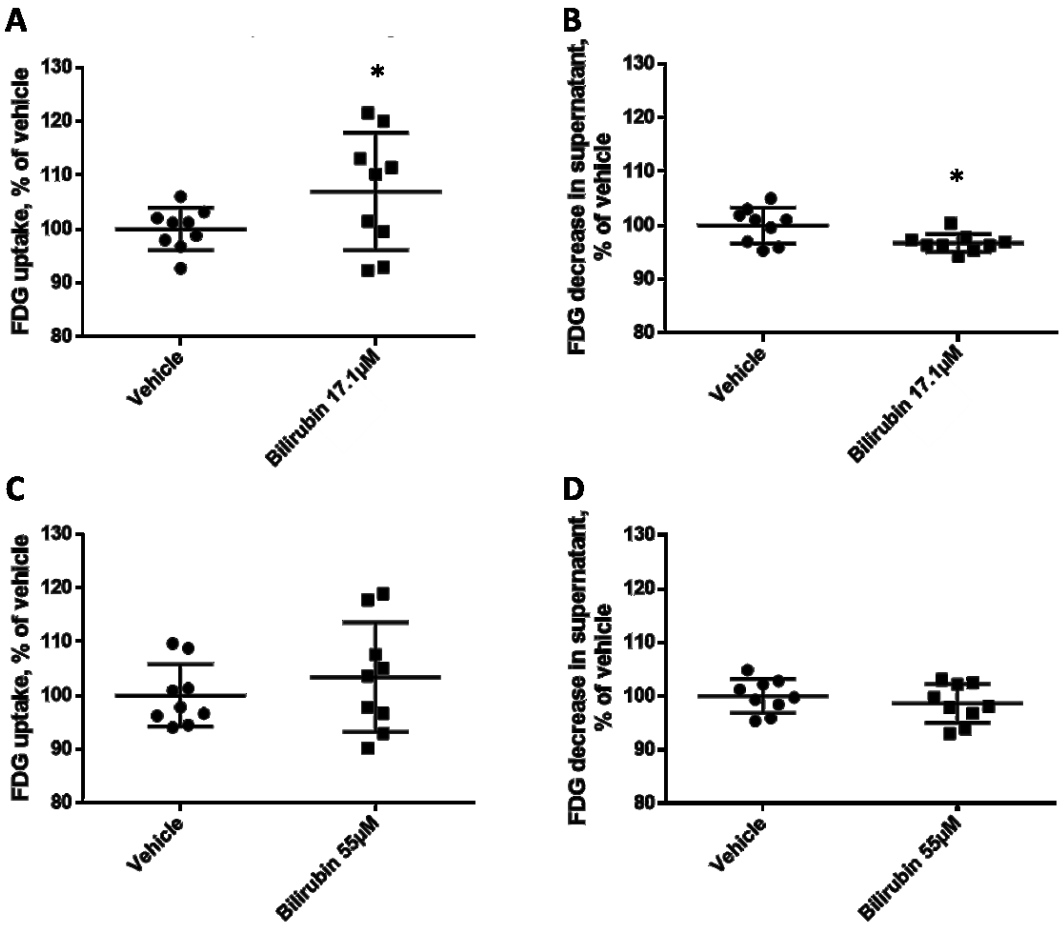

Figure 18: Uptake of [^{18}F]FDG in cellular fractions and decrease of [^{18}F]FDG in the supernatant after treatment with +Glu for 5 hours and -Glu for 2 hours in HepG2: A) results after treatment with 17.1µM UCB in cellular fractions (p=0.09), B) results after treatment with 17.1µM UCB in the supernatant (p=0.02), C) results after treatment with 55µM UCB in cellular fractions (p=0.40) and D) results after treatment with 55µM UCB in the supernatant (p=0.40)

4.1.1.3. 24 hours +Glu in C2C12

In the setting with an incubation of 24 hours, we aimed at a longer incubation time with UCB to perform a better approach to the chronic condition in GS. After starving for 2 hours without glucose, an increased [^{18}F]FDG uptake in the cells as well as a decrease of [^{18}F]FDG in the supernatant was observed at both concentrations, i.e. 17.1µM UCB and 55µM UCB. Except the uptake of [^{18}F]FDG in the cellular fractions at 17.1µM UCB (figure 19A, p>0.05) these differences were found to be significant (figure 19B, p=0.004; figure 19C, p=0.009; figure 19D, p=0.007).

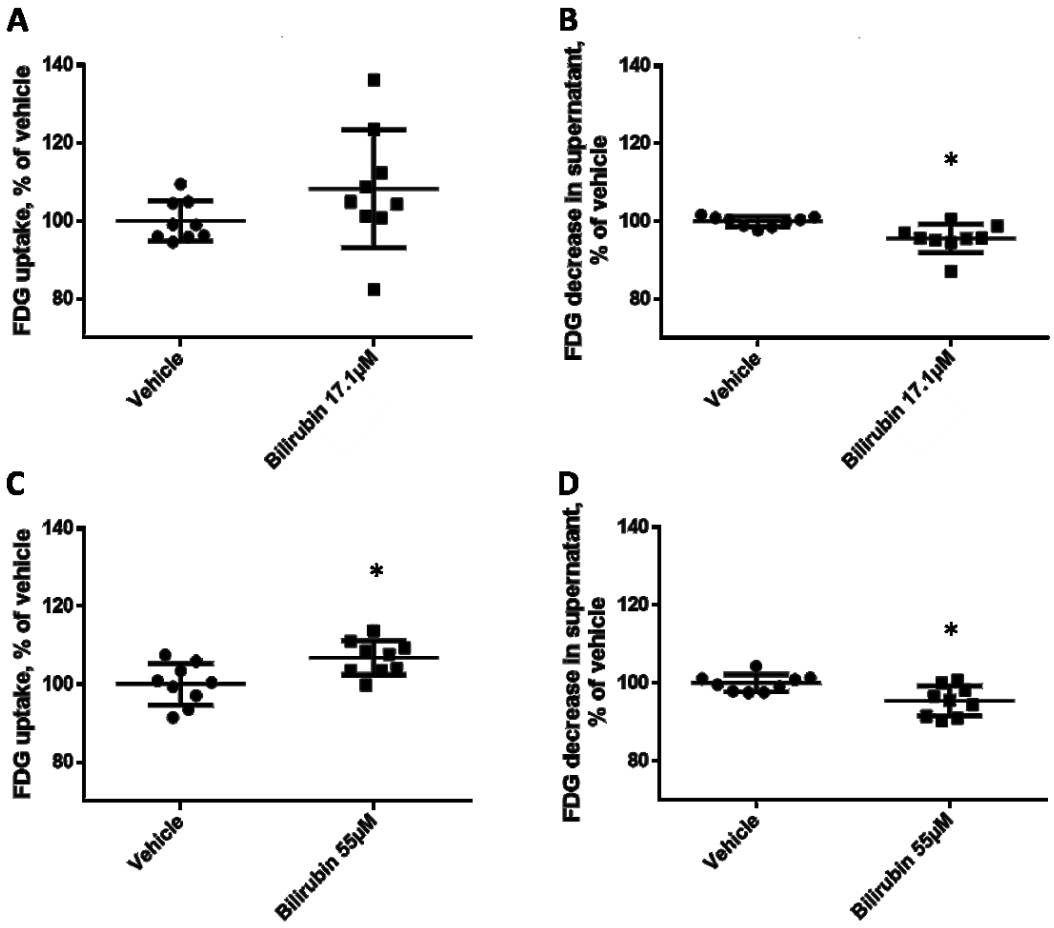

Figure 19: Uptake of [^{18}F]FDG in cellular fractions and decrease of [^{18}F]FDG in the supernatant after treatment with +Glu for 24 hours and -Glu for 2 hours in C2C12: A) results after treatment with 17.1µM UCB in cellular fractions (p=0.14), B) results after treatment with 17.1µM UCB in the supernatant (p=0.004), C) results after treatment with 55µM UCB in cellular fractions (p=0.009) and D) results after treatment with 55µM UCB in the supernatant (p=0.007)

4.1.1.4. 24 hours +Glu in HepG2

In the experiments with HepG2, the uptake of [^{18}F]FDG in the cellular fraction and the decrease in the supernatant showed a tendency towards our hypothesis following an incubation with 17.1µM UCB. At 17.1µM UCB, the [^{18}F]FDG uptake in the cellular fraction showed a strong trend and almost reached the level of significance (p=0.06), due to an outlier. However, this trend was not traceable after its exclusion or in the supernatant (Figure 20A and 20B, p>0.05). The effects observed after treatment with 55µM UCB were likewise not of statistical significance (figure 20C and 20D, p>0.05).

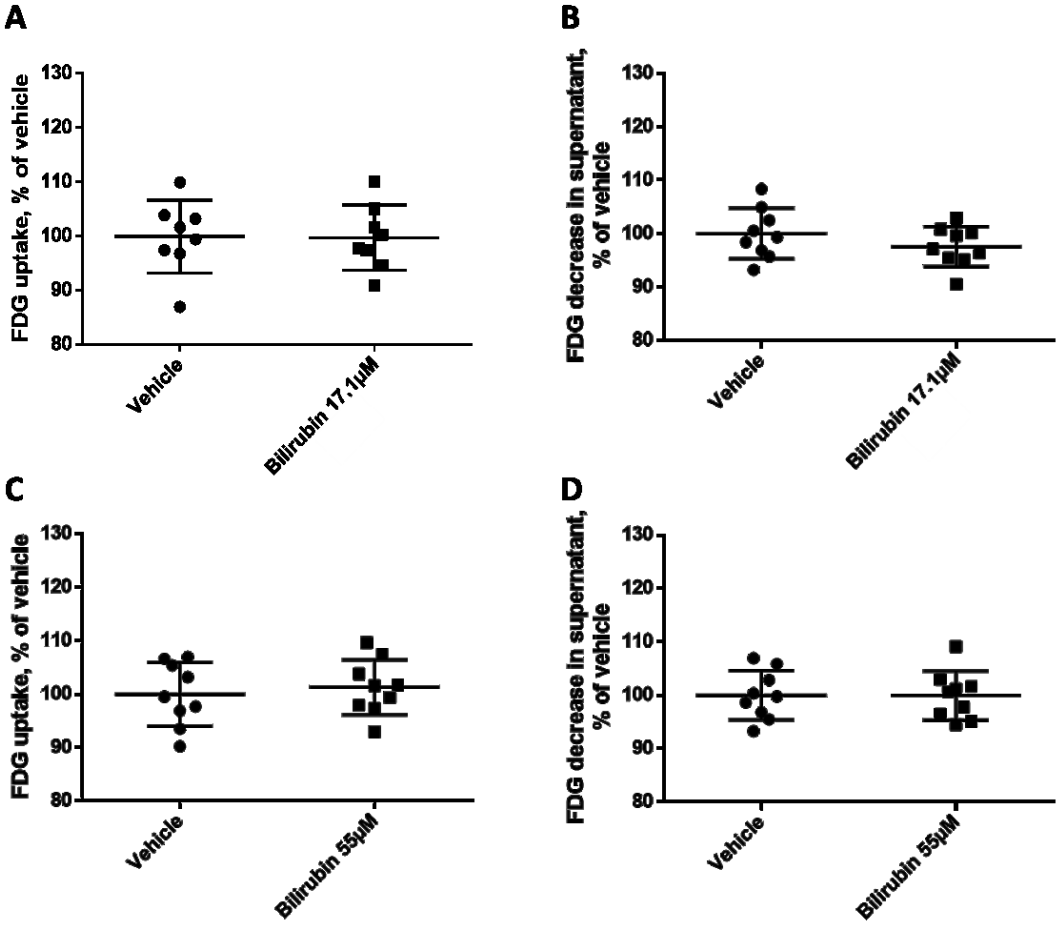

Figure 20: Uptake of [^{18}F]FDG in cellular fractions and decrease of [^{18}F]FDG in the supernatant after treatment with +Glu for 24 hours and -Glu for 2 hours in HepG2: A) results after treatment with 17.1µM UCB in cellular fractions (p=0.96), B) results after treatment with 17.1µM UCB in the supernatant (p=0.24), C) results after treatment with 55µM UCB in cellular fractions (p=0.62) and D) results after treatment with 55µM UCB in the supernatant (p=0.98)

4.2. [^{18}F]FDG Uptake with LigandTracer®

We further evaluated the kinetics of the [^{18}F]FDG uptake in C2C12 and HepG2 cells by LT technology. One of the advantages of this technology was the high sensitivity of the device. Moreover, the real-time assessment provides information on the kinetics of the uptake and generates plenty of valuable data. As described previously, the uptake of [^{18}F]FDG was analyzed after treatment with bilirubin or vehicle. The kinetics were assessed by adding the radioligand [^{18}F]FDG and measuring the uptake for 60 minutes. These real-time uptake studies

were conducted on both cell lines. The incubation times and concentrations of bilirubin were the same as in the well-plate experiments, i.e. 5 and 24 hours with 17.1 and 55µM UCB.

4.2.1. Treatment with glucose

4.2.1.1. 5 hours +Glu in C2C12

To qualitatively analyze the uptake of [^{18}F]FDG after 5 hours, the cells were incubated with UCB for 5 hours with +Glu following 2 hours UCB treatment with -Glu for starving. In line with our well-plate experiments of this setting, we could observe an increase in the uptake of [^{18}F]FDG after treatment with 17.1µM UCB (figure 21).

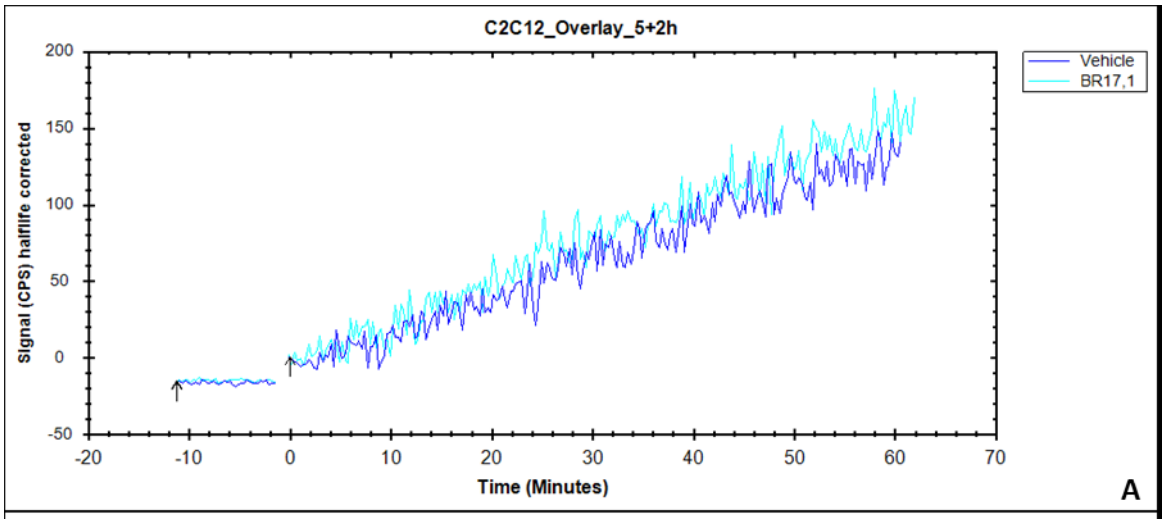

Figure 21: Comparison of the real-time uptake of [^{18}F]FDG in C2C12, treated 5 hours with +Glu and 2 hours with -Glu treatment: The overlay shows reference-subtracted binding curves, starting at minute 0 after 10 minutes of baseline, in comparison after treatment with vehicle (blue) or bilirubin (cyan). Different concentrations are shown, i.e. A) 17.1µM UCB

4.2.1.2. 5 hours +Glu in HepG2

The HepG2 cells showed an increased [^{18}F]FDG uptake in the cells after an incubation for 5 hours similarly to C2C12 cells uptake. The uptake in cells treated with 17.1µM UCB is markedly enhanced, compared to vehicle control (Figure 22A), which supports the results from our well-plate assay. However, the uptake after 55µM UCB treatment is lower than it is after 17.1µM treatment, which is in line with the results of the well plate assay (figure 22B). In this regard,

we have to point out that we were only able to perform the LT experiments once, in comparison to the well-plate assay, where we analyzed triplicates. Nonetheless, the LT is known for its extreme sensitivity, could be highly affected by daily conditions in the laboratory and therefore this result would need additional validation.

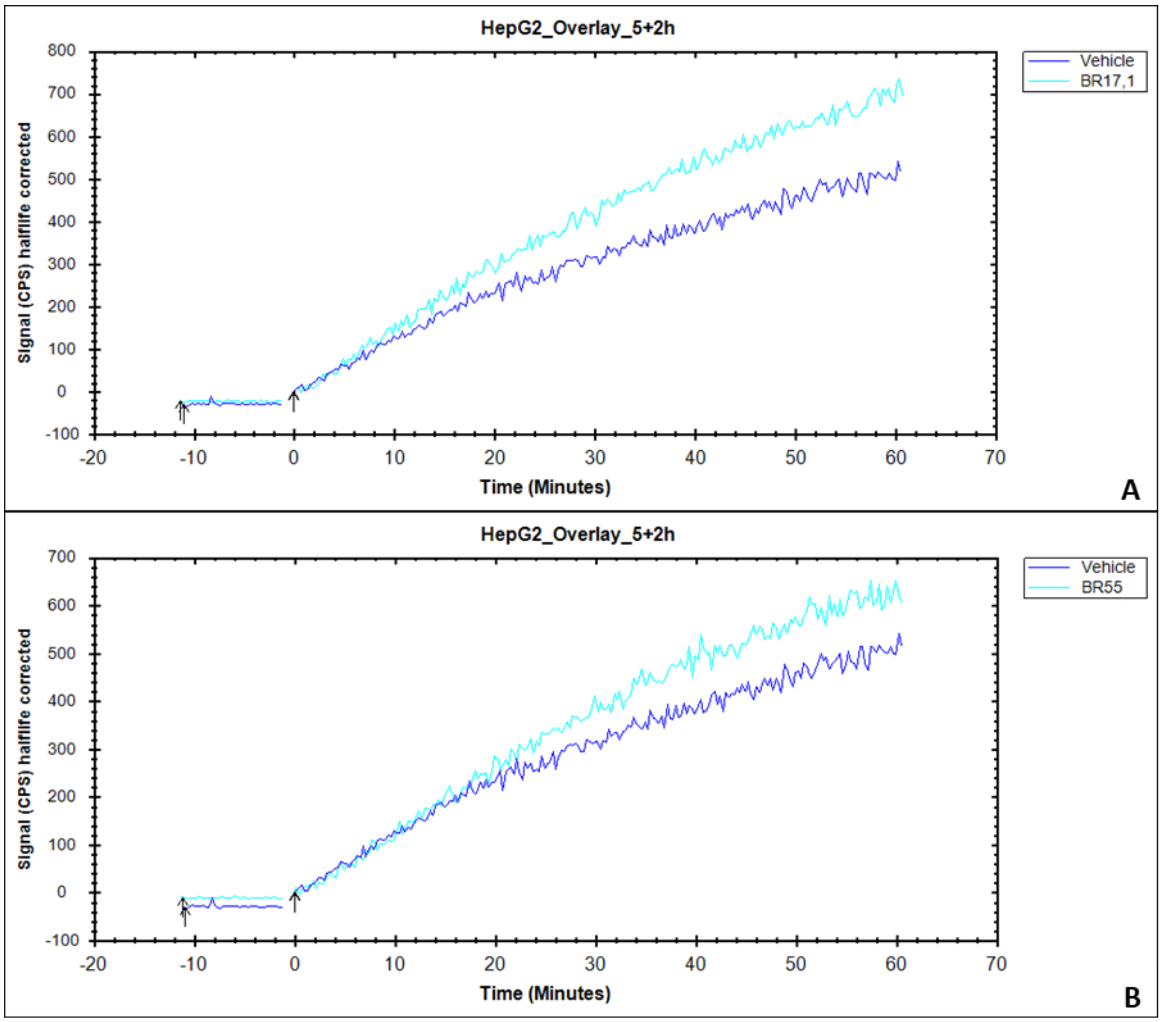

Figure 22: Comparison of the real-time uptake of [^{18}F]FDG in HepG2, treated 5 hours with +Glu and 2 hours with -Glu treatment: The overlay shows reference-subtracted binding curves, starting at minute 0 after 10 minutes of baseline, in comparison after treatment with vehicle (blue) or bilirubin (cyan). Different concentrations are shown, i.e. A) 17.1µM UCB and B) 55µM UCB

4.2.1.3. 24 hours +Glu in C2C12

Similar results as in HepG2 after 5 hours were obtained from C2C12 after 24 hours. A prolongation of the incubation time showed an increased uptake of [^{18}F]FDG after treatment with 17.1µM UCB (Figure 23A). These results are in line with the data we previously obtained.

However, an increase in UCB concentration to 55µM did not result in a more prominent glucose uptake, as shown in figure 23B. Since these findings are in contrast with the results from the well-plate assay, we have to mention the lack of repetition once more. Therefore, this overlay may not be representative and would need additional validation.

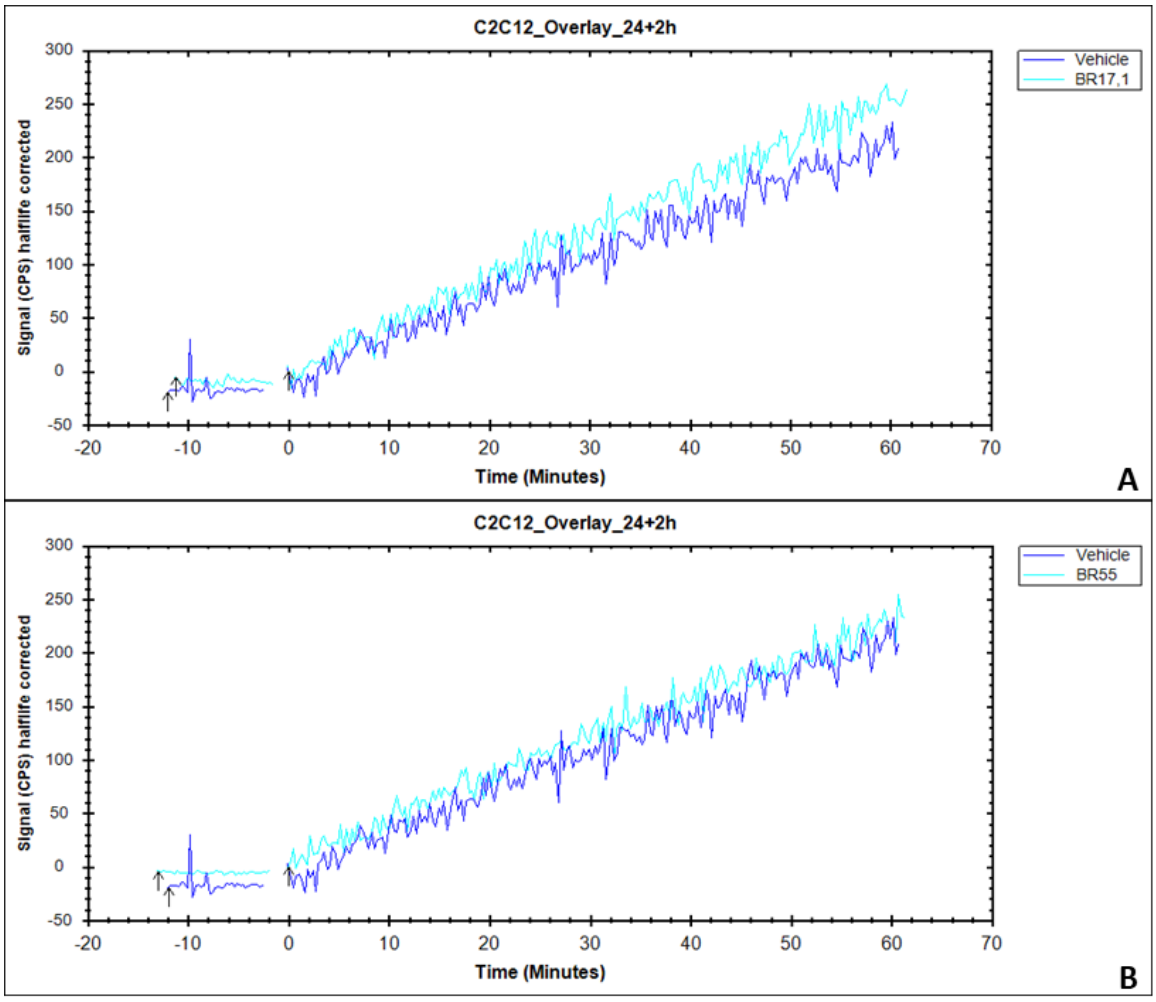

Figure 23: Comparison of the real-time uptake of [^{18}F]FDG in C2C12, treated 24 hours with +Glu and 2 hours with -Glu treatment: The overlay shows reference-subtracted binding curves, starting at minute 0 after 10 minutes of baseline, in comparison after treatment with vehicle (blue) or bilirubin (cyan). Different concentrations are shown, i.e. A) 17.1µM UCB, B) 55µM UCB

4.2.1.4. 24 hours +Glu in HepG2

The performance of the 24-hour setting with HepG2 supported our previous results from the well-plate assay. We were able to observe an increased uptake of [^{18}F]FDG after incubation

with 17.1µM UCB in comparison to vehicle (figure 24A), although it was clearly less distinct than after 5 hours of treatment. This increase was hardly detectable after incubation with 55µM UCB (Figure 24B). Therefore, we suggest a time- and dose-dependency in HepG2.

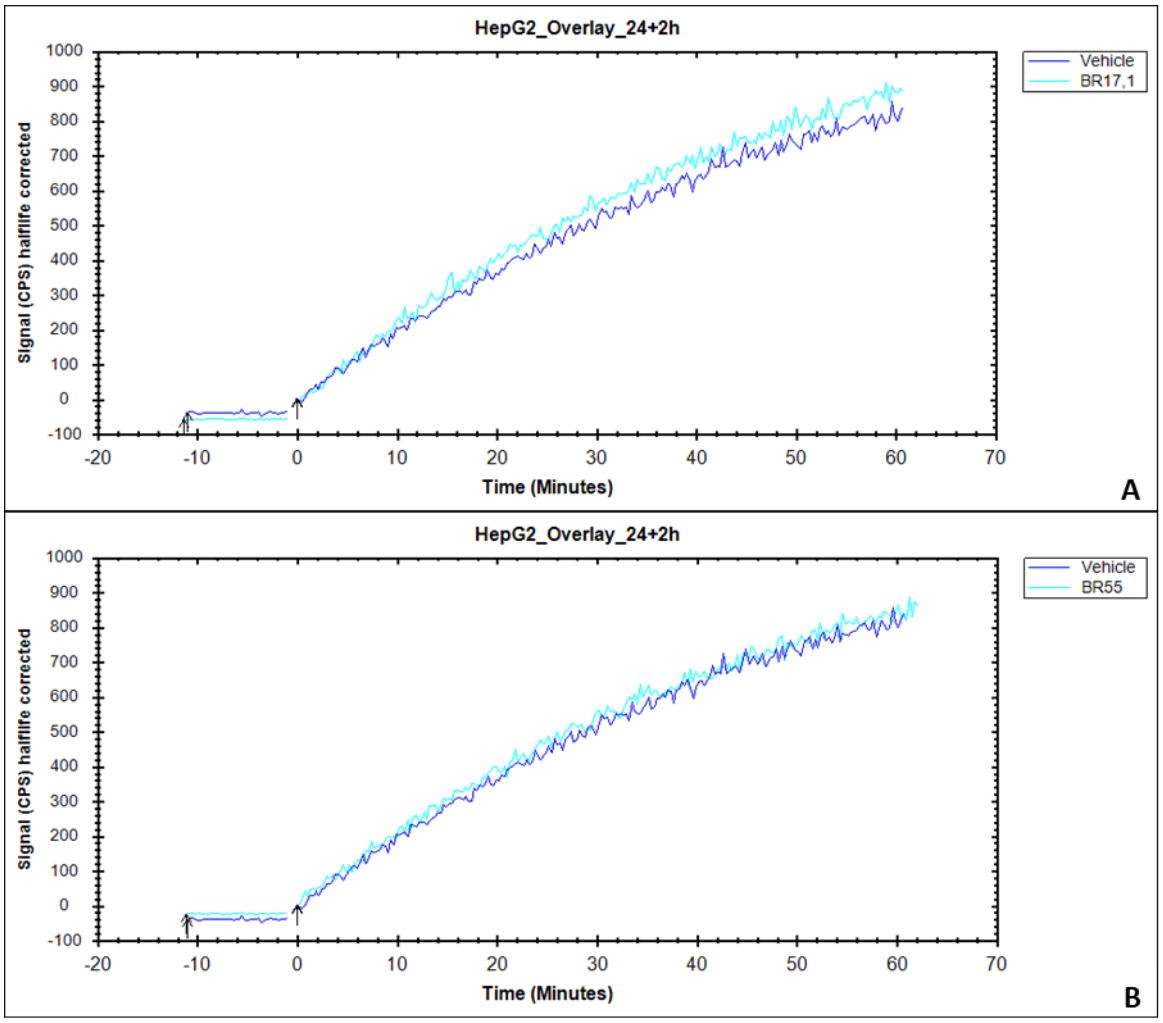

Figure 24: Comparison of the real-time uptake of [^{18}F]FDG in HepG2, treated 24 hours with +Glu and 2 hours with -Glu treatment: The overlay shows reference-subtracted binding curves, starting at minute 0 after 10 minutes of baseline, in comparison after treatment with vehicle (blue) or bilirubin (cyan). Different concentrations are shown, i.e. A) 17.1µM UCB, B) 55µM UCB

5. Method validation

During the establishment of the experimental settings for this study, several settings were examined. To evaluate the influence of UCB during a starving challenge on our cell lines, a setup without glucose during treatment was tested. Concentrations were similar to those used in the experiments with the addition of glucose during incubation with UCB. Starting with an incubation period of 5 hours, we were able to extend the incubation period up to 8 hours. However, according to previous cytotoxicity tests, further prolongation of treatment without glucose was not feasible, since in these settings glucose is necessary for the survival of the cells (unpublished data). Moreover, treatment with glucose is likely to be more similar to physiologic conditions in an organism, where a continuous supply of glucose is provided. Nevertheless, also in these experiments effects of UCB on [^{18}F]FDG uptake were recorded as shown in the detailed description below.

5.1. Additional settings of the 6-well-plate assay

5.1.1. 5 hours -Glu in C2C12

In the experiments with an incubation of 5 hours in glucose free UCB treatment, a slight increase in [^{18}F]FDG uptake in the cells as well as a decrease in the supernatant was found. This increase of [^{18}F]FDG uptake was not significant in the cell fractions of C2C12, regardless of the concentration of bilirubin (figure 25A, 25C, $p>0.05$). The decrease of [^{18}F]FDG was found to be significant in the supernatant after incubation with a concentration of 17.1µM UCB (figure 25B, $p=0.01$). However, this significance was not seen after incubation with a concentration of 55µM UCB (figure 25D, $p>0.05$).

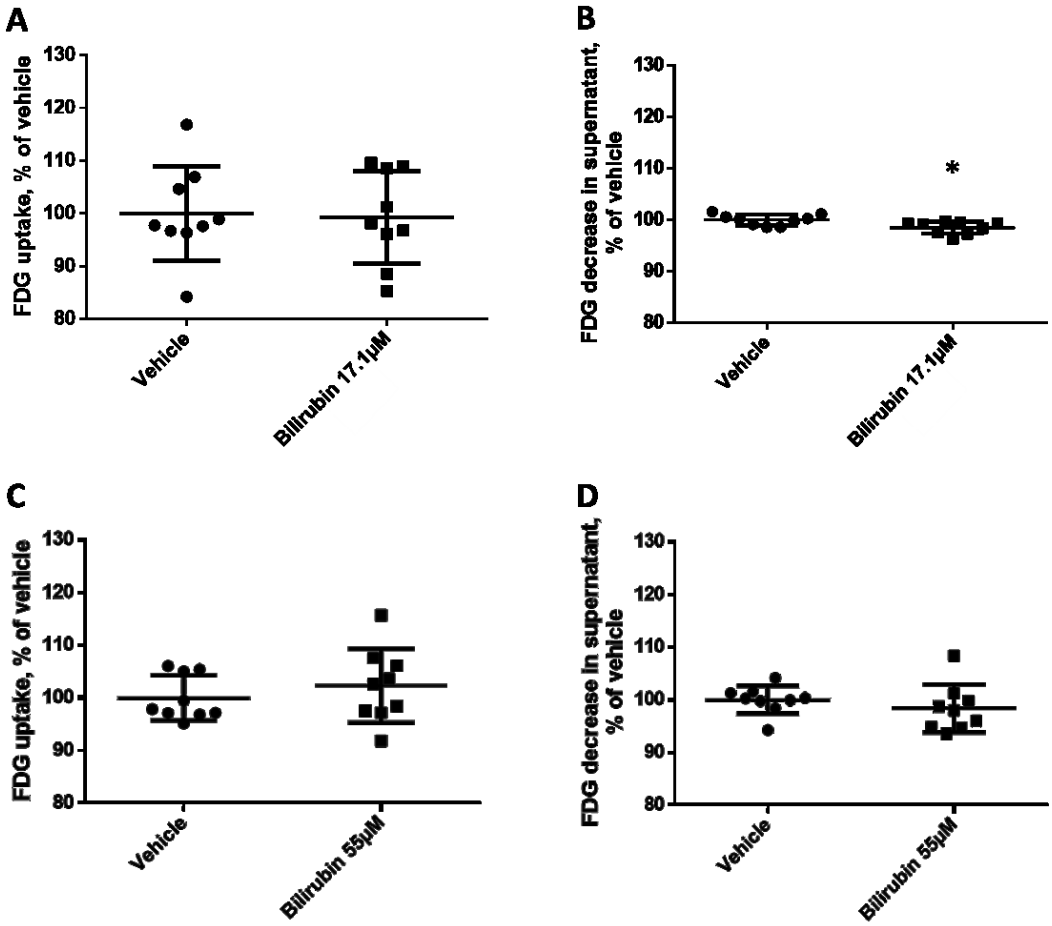

Figure 25: Uptake of [^{18}F]FDG in cellular fractions and decrease of [^{18}F]FDG in the supernatant after treatment with -Glu for 5 hours in C2C12: A) results after treatment with 17.1µM UCB in cellular fractions (p=0.86), B) results after treatment with 17.1µM UCB in the supernatant (p=0.01), C) results after treatment with 55µM UCB in cellular fractions (p=0.42) and D) results after treatment with 55µM UCB in the supernatant (p=0.36)

5.1.2. 5 hours -Glu in HepG2

When repeating the 5-hour setting with HepG2, no significant effects of bilirubin incubation were found. Thus, these results did not support our hypothesis. In particular, the cellular fraction showed no difference after treatment with 17.1µM UCB (Ffgure 26A, p>0.05). Neither did the supernatant after treatment with both concentrations (figure 26B and 26D, p>0.05). Moreover, there was an almost significant decrease of glucose uptake in the cellular fraction after treatment with 55µM UCB (Figure 26C, p=0.06). In the light of the results found in the C2C12 cells, it is tempting to speculate that the functional differences in the metabolisms

might be responsible for the differences in the results. Cellular stress induced by the lack of glucose during treatment also has to be considered.

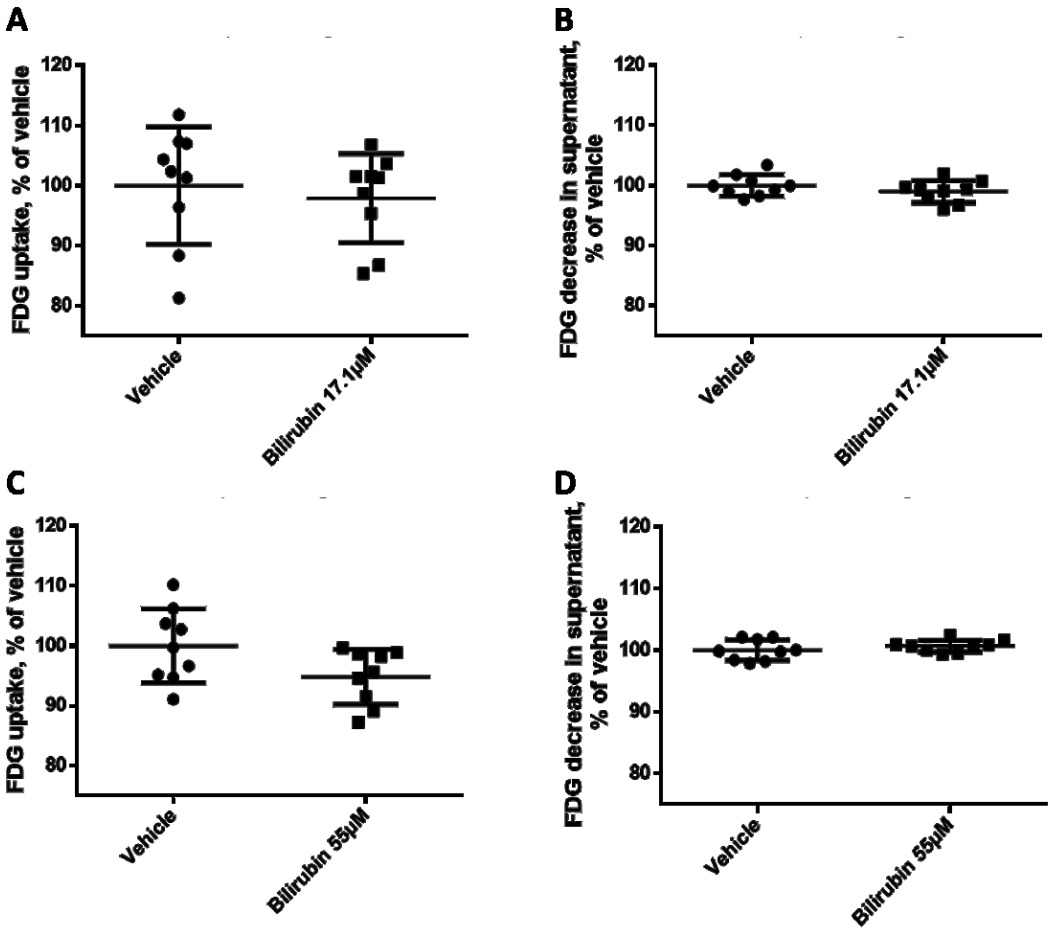

Figure 26: Uptake of [^{18}F]FDG in cellular fractions and decrease of [^{18}F]FDG in the supernatant after treatment with -Glu for 5 hours in HepG2: A) results after treatment with 17.1µM UCB in cellular fractions (p=0.61), B) results after treatment with 17.1µM UCB in the supernatant (p=0.25), C) results after treatment with 55µM UCB in cellular fractions (p=0.06) and D) results after treatment with 55µM UCB in the supernatant (p=0.33)

5.1.3. 8 hours -Glu in C2C12

In C2C12 cells an incubation with 55µM UCB for 8 hours without glucose resulted in an increase of [^{18}F]FDG uptake in the cells. The higher absorption of [^{18}F]FDG led to a decrease in the supernatant. In these experiments, both, the elevated uptake of [^{18}F]FDG in the cells as

well as the decrease of [^{18}F]FDG in the supernatant were found to be statistically significant (figure 27A, p=0.03; Figure 27B, p=0.02).

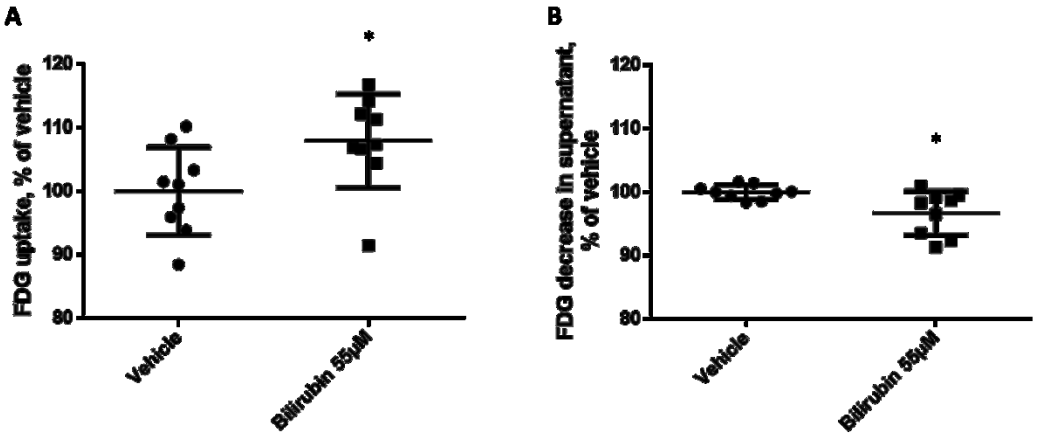

Figure 27: Uptake of [^{18}F]FDG in cellular fractions and decrease of [^{18}F]FDG in the supernatant after treatment with -Glu for 8 hours in C2C12: A) results after treatment with 55µM UCB in cellular fractions (p=0.03), B) results after treatment with 55µM UCB in the supernatant (p=0.02)

5.1.4. 8 hours -Glu in HepG2

Again, the same setting (i.e. incubation with UCB for 8 hours without glucose) in HepG2 cells did not support our hypothesis. In the 17.1µM concentration there was no difference detectable between vehicle and UCB-treatment neither in cellular fraction, nor in supernatant and no level of significance was reached (figure 28A and 28B, p>0.05). Treatment of the cells with 55µM UCB resulted in decrease of glucose uptake in the cellular fraction. In line, there was a slight increase of [^{18}F]FDG visible in the supernatant after treatment compared to vehicle control. The decrease in the cells was statistically significant (figure 28C, p=0.002) whereas the difference in the supernatant was not significant (figure 28D, p>0.05).

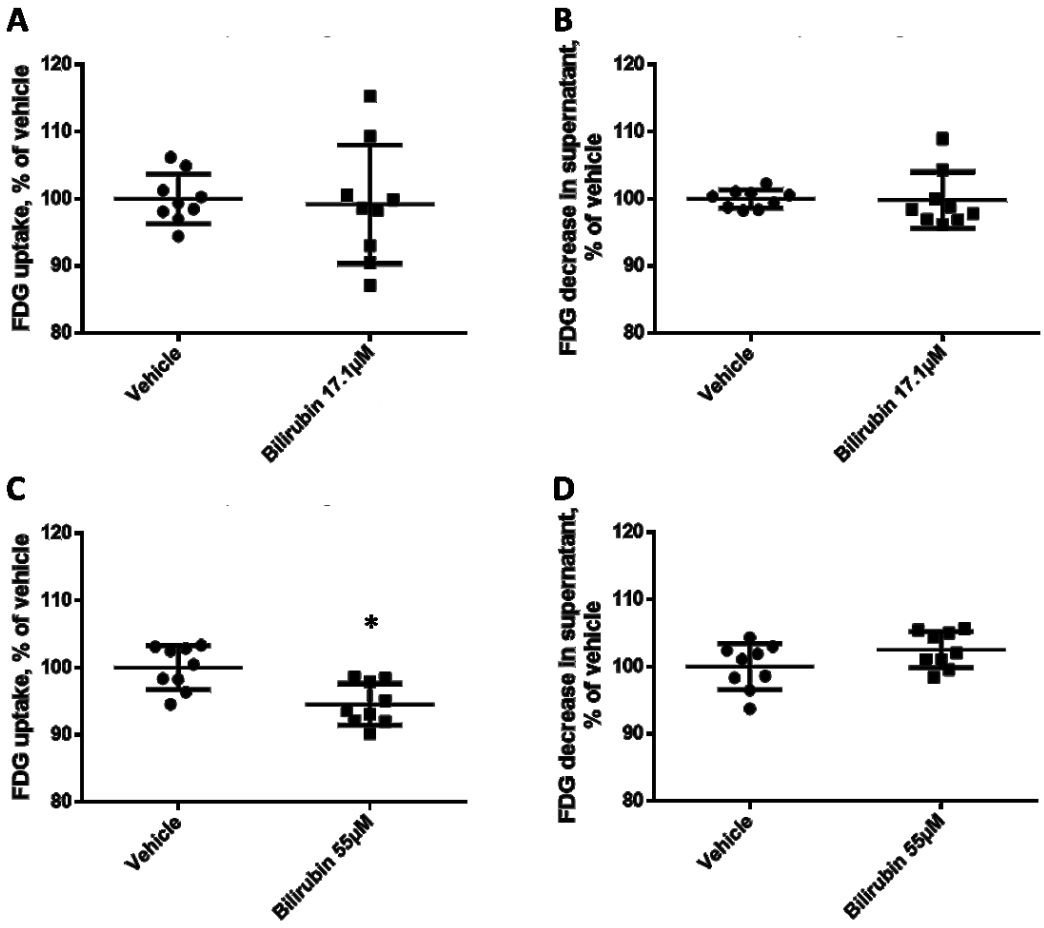

Figure 28: Uptake of [^{18}F]FDG in cellular fractions and decrease of [^{18}F]FDG in the supernatant after treatment with -Glu for 8 hours in HepG2: A) results after treatment with 17.1µM UCB in cellular fractions (p=0.80), B) results after treatment with 17.1µM UCB in the supernatant (p=0.90), C) results after treatment with 55µM UCB in cellular fractions (p=0.002) and D) results after treatment with 55µM UCB in the supernatant (p=0.10)

5.2. Additional settings of the LigandTracer® assay

5.2.1. 5 hours -Glu in C2C12

Figure 29 shows the binding curves of the setting after 5 hours incubation without glucose. In these experiments, an increased uptake of [^{18}F]FDG in C2C12 cells was observed after incubation with bilirubin. The incubation with both concentrations 17.1µM (Figure 29A) and 55µM UCB (Figure 29B) resulted in a markedly increased [^{18}F]FDG uptake in the cells treated with UCB compared to vehicle control.

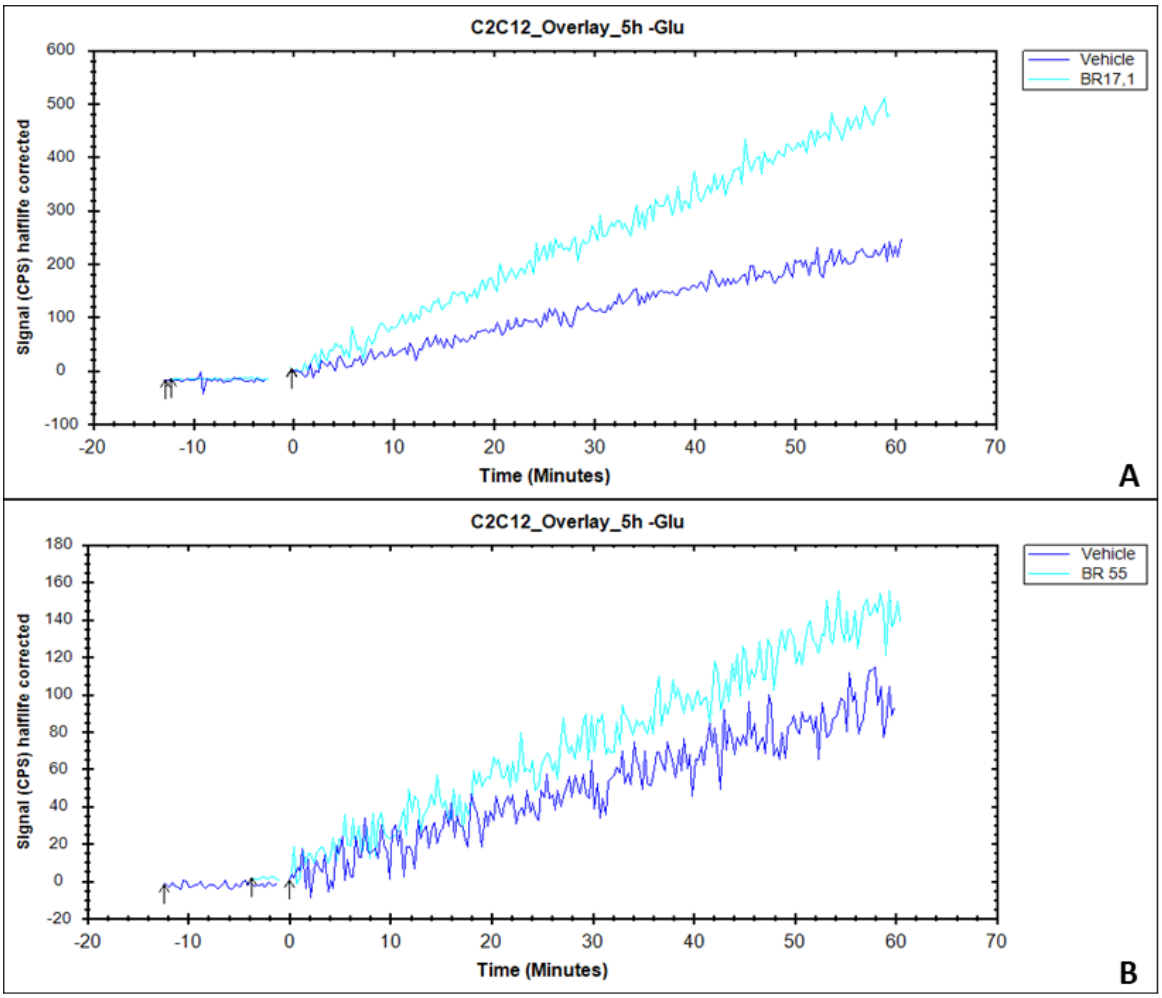

Figure 29: Comparison of the real-time uptake of [^{18}F]FDG in C2C12, treated 5 hours with -Glu treatment: The overlay shows reference-subtracted binding curves, starting at minute 0 after 10 minutes of baseline, in comparison after treatment with vehicle (blue) or bilirubin (cyan). Different concentrations are shown, i.e. A) 17.1µM UCB and B) 55µM UCB.

5.2.2. 5 hours -Glu in HepG2

In experiments using the cell line HepG2, similar results were obtained in the 5 hours -Glu setting as in C2C12. The [^{18}F]FDG uptake was increased in the cells treated with UCB compared to vehicle control (figure 30). These results were observed in both concentrations, i.e. 17.1µM UCB (figure 30A) and 55µM (figure 30B).

To analyze time dependent effects of bilirubin, the incubation time was prolonged from 5 hours to 8 hours. Unfortunately, this duration exceeded the feasible time period for the performance of the LigandTracer® assay in this project, since two dishes have to be measured

after each other on the same day. Hence, this setting was only performed in the 6-well-plate assay.

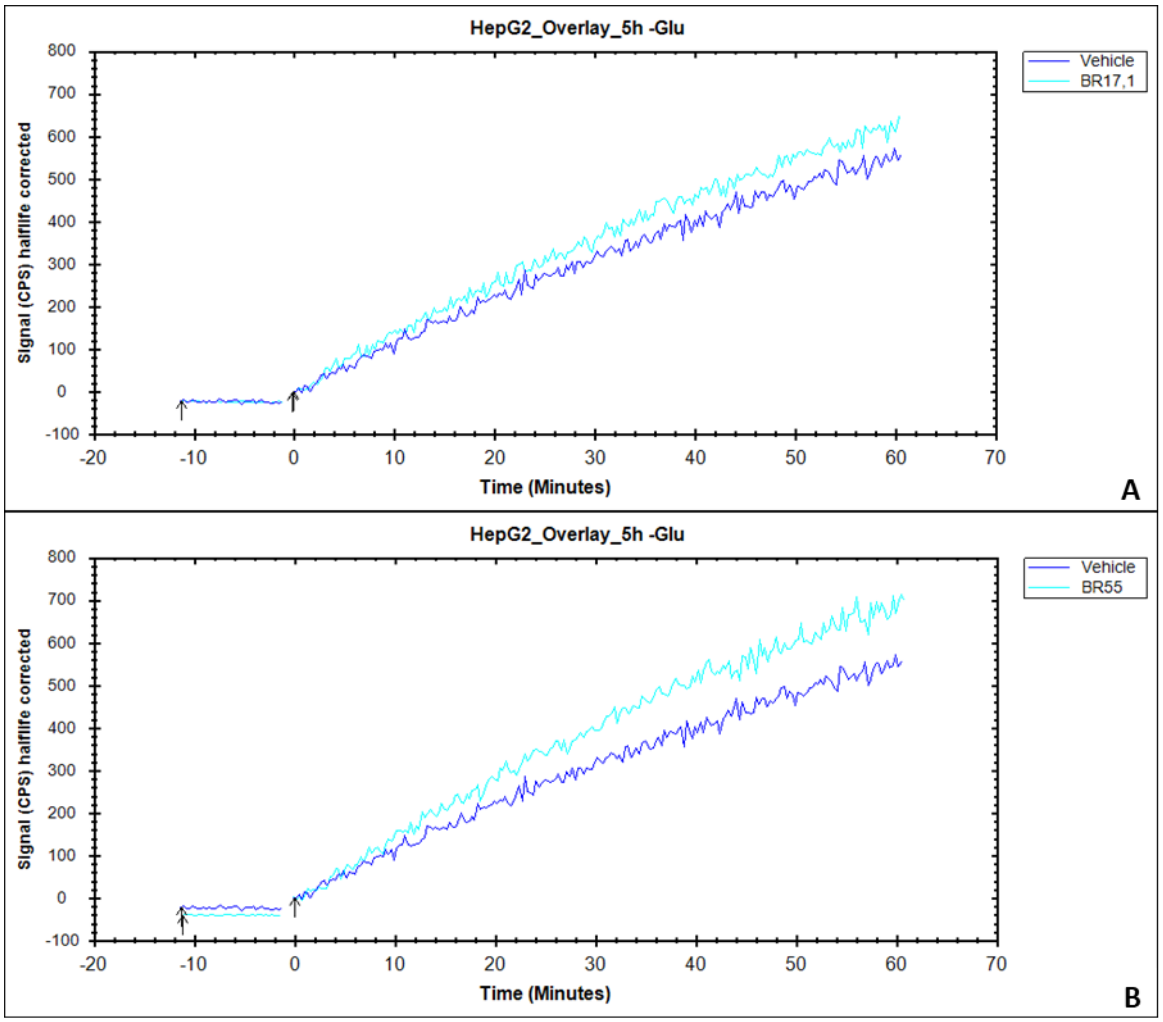

Figure 30: Comparison of the real-time uptake of [^{18}F]FDG in HepG2, treated 5 hours with -Glu treatment: The overlay shows reference-subtracted binding curves, starting at minute 0 after 10 minutes of baseline, in comparison after treatment with vehicle (blue) or bilirubin (cyan). Different concentrations are shown, i.e. A) 17.1µM UCB, B) 55µM UCB

6. Discussion

A number of recently published papers provide evidence that mildly elevated bilirubin concentrations are protective against disorders induced by oxidative stress (83). Among these, atherosclerotic conditions including cardiovascular disorders, arterial occlusive disease, and ischemic cerebrovascular disease are those to be most clinically relevant. Likewise, there are clinical studies to demonstrate an increased risk of coronary heart disease as well as peripheral vascular disease in subjects with low serum bilirubin levels (83). Another risk factor for atherosclerosis in nowadays society is the elevation of glucose levels in the peripheral blood (83). In GS individuals, known to have a lower risk for CVD compared to non-GS individuals, serum glucose levels were also found to be lower. In this regard one could speculate that mild elevation of bilirubin might result in an increased uptake of glucose in various cells of an organism. This could be due to an increased energy metabolism and therefore an enhanced need for macronutrients such as glucose (5). Indeed, Liu et al. found a regulation of the cholesterol metabolism and adipokines by bilirubin. This is likely to contribute to an increased insulin sensitivity and glucose tolerance, found in diet-induced obese (DIO) mice (84). These findings are supported by the results of Dong et al. who reported an increasing insulin sensitivity after bilirubin administration in both genetically engineered and DIO mice (85).

Thus, in our project we were interested in evaluating whether bilirubin was able to increase the uptake of glucose in muscle and liver cells. Therefore, an experimental setting was established to measure the influence of UCB on the uptake of [^{18}F]FDG in the murine muscle cell line C2C12 and hepatocarcinoma derived cell line HepG2. We hypothesized a potential increase in cellular uptake of [^{18}F]FDG in the cells and a respective decrease in the supernatant after treatment with 17.1µM and 55µM UCB. Therefore, research was performed using a conventional uptake assay and a very sensitive real-time assay for qualitative analysis. In the skeletal muscle cell line C2C12 we observed clearly positive results towards our hypothesis. In particular, there was an increase of [^{18}F]FDG uptake in the cells after incubation with UCB at low and high concentrations, i.e. 17.1µM and 55µM, respectively. These results were found after a treatment period of 5 and 24 hours. These data were confirmed by a decrease of [^{18}F]FDG in the supernatant of these cells. The kinetic of the [^{18}F]FDG uptake was analyzed using LT technology. The results obtained in these experiments were in line with the data of the 6-well-plate assay and thus, supported our hypothesis. Overall, the uptake of [^{18}F]FDG

after UCB-treatment was more prominent in the C2C12 cells as compared to the hepatocellular carcinoma cells HepG2. Whereas in the muscle cell line the uptake was elevated in all experimental settings, we observed an increase of [^{18}F]FDG uptake in HepG2 cells only at low UCB concentration after a short incubation time, i.e. 17.1µM for 5 hours. No increase was found at higher concentrations of UCB or after prolonged incubation.

Thus, the data obtained in the liver cells seem to be in contrast to the results observed in the muscle cells. In this regard, it has to be mentioned that u-shaped effects of bilirubin are discussed for example in CVD (86) and therefore 55µM might result in different effects then the lower concentration, particularly in the liver. Furthermore, these in part contradicting results might also be explained by the different physiologic properties of the cells, reflecting the metabolic demands of liver and muscle. A possible explanation could be the differences in the metabolism of glucose and therefore glycogen. First, an example reflecting the differential functions of liver and muscle in their metabolism of glycogen are the tissue-specific enzymatic isoforms for the regulation of the glucose and glycogen metabolism. Therefore, different isoforms of the glycogen synthase and phosphorylase are expressed in these cells (39). Their regulation shows a number of similarities, but there are also substantial differences in the sensitivity for allosteric regulators of these enzymes. Second, the major glucose transporter used in the liver and the muscle differs. In the liver GLUT2 is expressed in the membrane (41,42). It has a rather low affinity for glucose (39). In muscle cells GLUT4 is the major glucose transporter, known to express a high affinity for glucose (39,43). These previously published data could explain our findings of an increase of [^{18}F]FDG uptake only at moderately elevated, intracellular UCB accumulation in hepatocytes.

Interestingly, the results obtained in the LT experiments did not differ substantially between C2C12 and HepG2 cells. Here UCB induced an elevated [^{18}F]FDG uptake in both cell lines. In this regard we have to point out that the LT yellow is a highly sensitive device. In this assay, smaller effects can result in detectable differences in the [^{18}F]FDG uptake. Thus, the detection of an elevation in the [^{18}F]FDG uptake in the LT assay could be explained by the higher sensitivity of the assay. However, considering the differences in their sensitivity, both experimental approaches show that treatment with UCB elevates the uptake of [^{18}F]FDG. Therefore, also the LT experiments confirmed our hypothesis that bilirubin induces an increased glucose uptake in cells.

Another point to be considered in the discussion of our results is the experimental setting. We performed an *in vitro* study to investigate basic research on the effects of bilirubin. The results of our experiments seem to indicate that bilirubin contributes to an increased glucose uptake. However, the experimental setting does not fully represent the conditions present *in vivo*. Our cells were treated with UCB for a maximum duration of 24 hours. In GS individuals UCB is elevated after developing GS usually after adolescence, around the age of 18 years and older (9). The cells of their organism are continuously exposed to mildly elevated bilirubin. Thus, in this chronic condition the potential beneficial and protective effects regarding CVD, overweight and diabetes might also be a product of this long-term exposition to mild hyperbilirubinemia. It is tempting to speculate that such a long-term exposition might be necessary to induce further metabolic changes in the cells. Therefore, an early exposure of the proliferating and differentiating cells to UCB might be of interest. In such experiments UCB treatment would last several days to weeks and could enable the cells to fully develop different enzymatic features compared to cells treated with UCB only for several hours. Our observation of a significant increase of [^{18}F]FDG uptake already after short- to mid-term exposure could be a first step towards this approach which should be addressed in future studies.

Furthermore, regarding our project we were only able to investigate the effects of UCB on murine muscle cells and human hepatocarcinoma cells. However, in an organism there is a complex interplay among different cell types. In this regard, also other cells might be an important target for UCB. Indeed, there are data from studies similar to our project, suggesting that bilirubin may also influence other cell lines. For example, He et al. investigated the protection by HO-1-derived bilirubin of bovine endothelial cells against high glucose-induced damage (87). In addition, Clark et al. conducted experiments with vascular smooth muscle cells and their findings provide evidence that bilirubin has an impact on the cytoprotection against oxidative stress (88). In another *in vitro* study by Peyton et al. the ability of bilirubin to regulate the proliferation and migration of human arterial smooth muscle cells was examined (89). Alike these studies, our project elucidates an aspect of the complex interplay of bilirubin. Altogether, already published data on the effects of bilirubin on various cell types provide further evidence on the protective effect of mildly elevated bilirubin.

To further analyze the different aspects of the potential protective effects in a setting that would reflect the *in vivo* situation even better would be of interest. Therefore, the next step would be to reproduce the data obtained from our *in vitro* setting in a model organism. In such an organism, different effects on various cell types and their interaction with each other could be studied. These cell-cell interactions are of importance for the development and function of multicellular organisms (90). Hence, the effect of UCB could exhibit itself differently considering a whole organism. Since GS is associated with a promoter variation of UGT1A1 (9,17,30), one could possibly think of introducing the TA-insertion mutation in the TATA box of a knock-in mouse model or GUNN rats. This would be according to the polymorphic mutation UGT1A1*28 and UGT1A1*6, representing two of the most common polymorphisms in GS (9). By this it would be possible to further substantiate our hypothesis.

7. Conclusion

Studies with [^{18}F]FDG proved to be a useful tool to investigate the effect of the bile pigment bilirubin on glucose uptake in the two cell lines C2C12 and HepG2. Therefore, research was performed using a conventional uptake assay. The [^{18}F]FDG uptake showed an increase after the incubation with UCB. In particular, UCB significantly increased the uptake of [^{18}F]FDG in C2C12 after an incubation with 17.1µM and 55µM UCB respectively. These effects were observed after treatment periods of 5 and 24 hours. In HepG2 a significant increase in the uptake of [^{18}F]FDG was found only after an incubation with 17.1µM UCB for 5 hours. This effect could not be detected at high UCB concentrations or after a prolongation of UCB incubation.

In addition, the uptake kinetics of [^{18}F]FDG uptake after UCB incubation was examined by LigandTracer® technology in a very sensitive real-time assay for qualitative analysis. Also in this assay the results have shown a clear uptake of [^{18}F]FDG after incubation with UCB. This uptake was markedly higher in comparison to cells incubated with a vehicle control treatment. Hence, the data obtained previously in the conventional uptake assay could be confirmed with these real-time uptake studies.

Our results support the hypothesis that UCB increases the uptake of glucose in C2C12 and HepG2 cells. This could be a possible explanation for GS individuals being metabolically healthier than non-GS individuals. Conclusively, our project supports the recent approach to see bilirubin in a new and more positive light. It is no longer only cytotoxic at high levels and a sign of disease as seen in patients with liver disorders. As shown in this study as well as in previous reports, bilirubin is also a protective factor against various disorders associated with vascular damage, when levels are elevated mildly and therefore a renewed approach to benign hyperbilirubinemia should be achieved.

8. Abstract

Background: Recently it has been shown that mildly elevated bilirubin concentrations, as present in individuals with Gilbert's syndrome (GS), are protective against disorders induced by oxidative stress including cardiovascular disorders or arterial occlusive disease. The aim of the present study was to analyze whether unconjugated bilirubin (UCB) was able to increase the uptake of glucose in muscle and liver cells.

Methods: For our experiments, the murine muscle cell line C2C12 and hepatocarcinoma derived cell line HepG2 were used in a well-plate assay. Cells were incubated with UCB for 5 and 24 hours at concentrations analogously to physiological blood concentrations (17.1µM and 55µM) or vehicle control. After glucose starving for 2 hours, to ensure a proper uptake, 150 kBq of 2-[^{18}F]fluoro-2-deoxy-D-glucose ([^{18}F]FDG), a glucose analogue with the positron-emitting radionuclide fluorine-18, was added for 1 hour. Finally, the uptake of [^{18}F]FDG in cell fractions and the supernatant, was measured using 2480 Wizard² Automatic Gamma Counter. In addition, the [^{18}F]FDG uptake in the cell lines was measured by a real-time uptake assay with LigandTracer® (LT) technology.

Results: In the skeletal muscle cell line C2C12 we observed a significant increase of [^{18}F]FDG uptake in the cells after incubation with 17.1µM and 55µM UCB for 5 and 24 hours. As assessed by LT technology, the kinetics of the [^{18}F]FDG uptake were in line with the data obtained from the well-plate assay. Overall, the uptake of [^{18}F]FDG after UCB-treatment was more prominent in the C2C12 cells as compared to the hepatocellular carcinoma cells HepG2. We observed an increase of [^{18}F]FDG uptake in HepG2 cells after incubation with 17.1µM UCB for 5 hours. No increase was found at higher concentrations of UCB or after prolonged incubation in this cell line. The weaker effect of UCB on the liver cells could be explained by a different metabolism of glucose in muscle and liver cells, reflecting the differential functions of these tissues.

Conclusion: Our results provide evidence that UCB improves the uptake of glucose in different types of cells. Therefore, they are in line with the recent approach to see bilirubin not only as a cytotoxic agent with mainly negative effects in severe hyperbilirubinemia, but also as a potential health-promoting factor. As clinically shown in GS individuals, mildly elevated bilirubin levels may also serve as a protective factor against various disorders, including cardio

vascular disorders. Our results offer further insights why GS individuals are metabolically healthier than non-GS individuals and should therefore be further investigated.

9. Zusammenfassung

Hintergrund: Seit kurzer Zeit befassen sich Forscher mit der Auswirkung von leicht erhöhten Bilirubinspiegeln, wie sie in Personen mit Gilbert Syndrom (GS) gefunden werden. Es hat sich gezeigt, dass diese milde Form der Hyperbilirubinämie eine protektive Wirkung gegenüber Erkrankungen hat, die durch oxidativen Stress verursacht werden, wie etwa kardiovaskuläre Erkrankungen oder arterielle Verschlusskrankheiten. Das Ziel unserer Studie war es die Auswirkungen von unkonjugiertem Bilirubin (UKB) auf die Glukose-Aufnahme in Muskel- und Leberzellen zu untersuchen.

Methodik: Für unsere Experimente wurden die murine Muskel-Zelllinie C2C12 und die humane Leberkarzinom-Zelllinie HepG2 verwendet. Um die Aufnahme des, mit dem Radionuklid Fluor-18 substituierten, Glukose-Analogs 2-[^{18}F]Fluor-2-desoxy-D-Glukose ([^{18}F]FDG) zu messen, wurde ein Well-Plate-Assay entwickelt. Hierfür wurden die Zellen für 5 und 24 Stunden mit einem Vehikel-Treatment oder mit Treatment mit UKB-Konzentration von 17,1µM und 55µM behandelt, wie sie auch in Personen mit GS vorliegen. Nachdem die Zellen anschließend für 2 Stunden ohne Glukose gefastet hatten, um eine adäquate Aufnahme [^{18}F]FDG zu garantieren, wurden den Zellen 150 kBq [^{18}F]FDG zugesetzt und für 1 Stunde inkubiert. Abschließend wurde die Aufnahme an [^{18}F]FDG separat in den Zell-Fragmenten und dem Überstand mittels 2480 Wizard² Automatic Gamma Counter gemessen. Zusätzlich zu dem Well-Plate-Assay wurde die Aufnahme an [^{18}F]FDG in diesen beiden Zelllinien noch in einem sensitiven Echtzeit-Assay mittels LigandTracer® (LT) Technologie evaluiert.

Ergebnisse: In der Muskel-Zelllinie C2C12 konnte eine signifikante Erhöhung der Aufnahme an [^{18}F]FDG nach Behandlung mit 17,1µM und 55µM UKB für 5 und 24 Stunden nachgewiesen werden. Die Daten der Aufnahme-Kinetik, die mittels LT Assay erhoben wurden, bestätigten diese Resultate. Generell war eine Erhöhung der [^{18}F]FDG -Aufnahme bei den C2C12 Zellen eindeutiger als bei den Leberkarzinom-Zellen HepG2. In diesen konnte eine signifikante Erhöhung der Aufnahme an [^{18}F]FDG nach Behandlung mit 17,1µM UKB für 5 beobachtet werden, nicht aber bei höheren UKB-Konzentrationen, oder einer verlängerten Inkubationszeit. Diese abgeschwächte Auswirkung von UKB könnte ihren Ursprung in den Unterschieden des Glukose-Stoffwechsels in Muskel- und Leberzellen und den jeweiligen unterschiedlichen Funktionen dieser Gewebe haben.

Conclusio: Die Ergebnisse unserer Studie liefern Hinweise darauf, dass UKB die Aufnahme von Glukose in verschiedenen Zelltypen erhöht. Damit unterstützen sie den rezenten Ansatz, nicht nur die zytotoxischen und negativen Auswirkungen stark erhöhter Bilirubin-Level, sondern auch potentielle gesundheitsfördernde Aspekte zu sehen. Wie bereits in Personen mit GS klinisch bewiesen werden konnte, zeigen leicht erhöhte Bilirubin-Level protektive Eigenschaften gegenüber verschiedene Erkrankungen, wie etwa kardiovaskulären Erkrankungen und unsere Ergebnisse geben einen weiteren Einblick, warum Personen mit GS metabolisch gesünder sind, als Personen ohne GS. Aus diesem Grund sollten unsere Forschungsergebnisse weiterverfolgt werden.

10. References

1. Wagner K-H, Wallner M, Mölzer C, Gazzin S, Bulmer AC, Tiribelli C, Vitek L. Looking to the horizon: the role of bilirubin in the development and prevention of age-related chronic diseases. Clin Sci [Internet]. 2015;129:1–25. Available from: http://clinsci.org/lookup/doi/10.1042/CS20140566

2. KLATSKIN G. Bile pigment metabolism. Annu Rev Med. 1961;12:211–50.

3. Kwon YJ, Lee YJ, Park BJ, Hong KW, Jung DH. Total serum bilirubin and 8-year incident type 2 diabetes mellitus: The Korean Genome and Epidemiology Study. Diabetes Metab [Internet]. Elsevier Masson SAS; 2017;1:2–9. Available from: http://dx.doi.org/10.1016/j.diabet.2017.07.004

4. Mölzer C, Wallner M, Kern C, Tosevska A, Zadnikar R, Doberer D, Marculescu R, Wagner KH. Characteristics of the heme catabolic pathway in mild unconjugated hyperbilirubinemia and their associations with inflammation and disease prevention. Sci Rep. 2017;7:1–15.

5. Mölzer C, Wallner M, Kern C, Tosevska A, Schwarz U, Zadnikar R, Doberer D, Marculescu R, Wagner KH. Features of an altered AMPK metabolic pathway in Gilbert's Syndrome, and its role in metabolic health. Sci Rep [Internet]. Nature Publishing Group; 2016;6:1–15. Available from: http://dx.doi.org/10.1038/srep30051

6. Seyed Khoei N, Grindel A, Wallner M, Mölzer C, Doberer D, Marculescu R, Bulmer A, Wagner KH. Mild hyperbilirubinaemia as an endogenous mitigator of overweight and obesity: Implications for improved metabolic health. Atherosclerosis. 2018;269:306–11.

7. Horsfall LJ. Serum Bilirubin and Risk of Respiratory Disease and Death. Jama [Internet]. 2011;305:691. Available from: http://jama.jamanetwork.com/article.aspx?doi=10.1001/jama.2011.124

8. Horsfall LJ, Nazareth I, Pereira SP, Petersen I. Gilbert's syndrome and the risk of death: a population-based cohort study. J Gastroenterol Hepatol [Internet]. 2013;n/a-n/a. Available from: http://doi.wiley.com/10.1111/jgh.12279

9. Wagner KH, Shiels RG, Lang CA, Seyed Khoei N, Bulmer AC. Diagnostic criteria and contributors to Gilbert's syndrome. Crit Rev Clin Lab Sci [Internet]. Informa Healthcare USA, Inc; 2018;55:129–39. Available from: https://doi.org/10.1080/10408363.2018.1428526

10. Bonnett R, Davies JE, Hursthouse MB, Sheldrick G. The Structure of Bilirubin. Proceeding R Soc London. 1978;202:249–68.

11. Vítek L, Ostrow JD. Bilirubin chemistry and metabolism; harmful and protective aspects. Curr Pharm Des. 2009;15:2869–83.

12. Heirwegh KPM, Fevery J, Blanckaert N. Chromatographic analysis and structure determination of biliverdins and bilirubins. J Chromatogr [Internet]. 1989;496:1–26. Available from: http://www.ncbi.nlm.nih.gov/pubmed/2687309

13. Wang X, Chowdhury JR, Chowdhury NR. Bilirubin metabolism: Applied physiology. Curr Paediatr. 2006;16:70–4.

14. Baranano DE, Rao M, Ferris CD, Snyder SH. Biliverdin reductase: A major physiologic cytoprotectant. Proc Natl Acad Sci [Internet]. 2002;99:16093–8. Available from: http://www.pnas.org/cgi/doi/10.1073/pnas.252626999

15. Itoh IS, Onishi S. Kinetic study of the photochemical changes of (ZZ)-bilirubin IXa bound. 1985;226:251–8.

16. Rigato I, Ostrow JD, Tiribelli C. Bilirubin and the risk of common non-hepatic diseases. Trends Mol Med. 2005;11:277–83.

17. Bulmer AC, Verkade HJ, Wagner KH. Bilirubin and beyond: A review of lipid status in Gilbert's syndrome and its relevance to cardiovascular disease protection. Prog Lipid Res [Internet]. Elsevier Ltd; 2013;52:193–205. Available from: http://dx.doi.org/10.1016/j.plipres.2012.11.001

18. Schmid R, McDonagh AF. The Enzymatic Formation of Bilirubin. Ann N Y Acad Sci. 1975;244:533–52.

19. Pimstone NR, Tenhunen R, Seitz PT, Marver HS, Schmid R. The enzymatic degradation of hemoglobin to bile pigments by macrophages. J Exp Med. 1971;133:1264–81.

20. Goessling W, Zucker SD. Role of apolipoprotein D in the transport of bilirubin in plasma. Am J Physiol Gastrointest Liver Physiol [Internet]. 2000;279:G356-65. Available from: http://www.ncbi.nlm.nih.gov/pubmed/10915645

21. Kamisako T, Kobayashi Y, Takeuchi K, Ishihara T, Higuchi K, Tanaka Y, Gabazza EC, Adachi Y. Recent advances in bilirubin metabolism research: The molecular mechanism of hepatocyte bilirubin transport and its clinical relevance. J Gastroenterol. 2000;35:659–64.

22. Vitek L, Kotal P, Jirsa M, Malina J, Cerná M, Chmelar D, Fervey J. Intestinal colonization leading to fecal urobilinoid excretion may play a role in the pathogenesis of neonatal jaundice. J Pediatr Gastroenterol Nutr. 200AD;30:294–8.

23. Strassburg CP. Hyperbilirubinemia syndromes (Gilbert-Meulengracht, Crigler-Najjar, Dubin-Johnson, and Rotor syndrome). Best Pract Res Clin Gastroenterol [Internet]. Elsevier Ltd; 2010;24:555–71. Available from: http://dx.doi.org/10.1016/j.bpg.2010.07.007

24. Chowdhury JR, Wolkoff A, Chowdhury NR, Arias I. Hereditary jaundice and disorders of bilirubin metabolism. In: Scriver C, Boudet A, Sly W, Valle D, editors. The metabolic and molecular bases of inherited disease. 8th ed. New York: McGraw Hill; 2001. p. 3063–101.

25. Bosma P, Roy Chowdhury N, Goldhoorn B, Hofker M, Oude Elferink R, Jansen P, Roy Chowdhury J. Rapid Communication Sequence of Exons and the Flanking Regions of Human Bilirubin-UDP-Glucuronosyltransferase Gene Complex and Identification of a Genetic Mutation in a Patient with Crigler-Najar Syndrome , Type I. Hepatology. 1992;15:941.

26. Ihara H, Hashizume N, Shimizu N, Aoki T. Threshold concentration of unbound bilirubin to induce neurological deficits in a patient with type I Crigler-Najjar syndrome. Ann Clin Biochem. 1999;36:347–52.

27. Ramírez J, Komoroski BJ, Mirkov S, Graber AY, Fackenthal DL, Schuetz EG, Das S, Ratain MJ, Innocenti F, Strom SC. Study of the genetic determinants of UGT1A1 inducibility by phenobarbital in cultured human hepatocytes. Pharmacogenet Genomics. 2006;16:79–86.

28. Wolkoff A, Wolpert E, Pascasio F, Arias I. Rotor's syndrome: a distinct inheritable pathophysiologic entity. Am J Med. 1976;60:173–9.

29. Gilbert A, Lereboulette P. La cholémie simple familiale. Sem Médicale. 1901;21:241–8.

30. Bosma PJ, Chowdhury JR, Bakker C, Gantla S, de Boer A, Oostra BA, Lindhout D, Tytgat GNJ, Jansen PLM, Elferink RPJO, et al. The Genetic Basis of the Reduced Expression of Bilirubin UDP-Glucuronosyltransferase 1 in Gilbert's Syndrome. N Engl J Med [Internet]. 1995;333:1171–5. Available from: http://www.nejm.org/doi/abs/10.1056/NEJM199511023331802

31. Chowdhury NR, Chowdhury JR. Disorders of bilirubin metabolism. The Liver: Biology and Pathobiology. 2009. p. 251–256.

32. Powell L, Hemingway E, Billing B, Sherlock S. Idiopathic Unconjugated Hyperbilirubinemia (Gilbert's Syndrome) — A Study of 42 Families. N Engl J Med. 1976;277:1108–12.

33. Powell L. Clinical aspects of unconjugated hyperbilirubinemia. Semin Hematol. 1972;9:91–105.

34. Stocker R, Yamamoto Y, McDonagh AF, Glazer AN, Ames BN. Bilirubin is an antioxidant of possible physiological importance. Science (80-). 1987;235:1043–6.

35. Vitek L, Jirsa M, Brodanova M, Kalab M, Marecek Z, Danzig V, Novotn?? L, Kotal P. Gilbert syndrome and ischemic heart disease: A protective effect of elevated bilirubin levels. Atherosclerosis. 2002;160:449–56.

36. S. S, Y.R. C, M.K. P, D.K. K, N.H. C, M.-K. L. Relationship between serum bilirubin levels and cardiovascular disease. PLoS One [Internet]. 2018;13:1–9. Available from: http://www.embase.com/search/results?subaction=viewrecord&from=export&id=L620727209%0Ahttp://dx.doi.org/10.1371/journal.pone.0193041

37. Vítek L. The role of bilirubin in diabetes, metabolic syndrome, and cardiovascular diseases. Front Pharmacol. 2012;3 APR:1–7.

38. Temme EHM, Zhang J, Schouten EG, Kesteloot H. Serum bilirubin and 10-year mortality risk in a Belgian population. Cancer Causes Control. 2001;12:887–94.

39. Greenberg CC. Glycogen branches out: new perspectives on the role of glycogen metabolism in the integration of metabolic pathways. AJP Endocrinol Metab [Internet]. 2006;291:E1–8. Available from: http://ajpendo.physiology.org/cgi/doi/10.1152/ajpendo.00652.2005

40. Calvo MB, Figueroa A, Pulido EG, Campelo RG, Aparicio LA. Potential role of sugar transporters in cancer and their relationship with anticancer therapy. Int J Endocrinol. 2010;2010.

41. Reske SN, Grillenberger KG, Glatting G, Port M, Hildebrandt M, Gansauge F, Beger HG. Overexpression of glucose transporter 1 and increased FDG uptake in pancreatic carcinoma. J Nucl Med. 1997;38:1344–8.

42. Lienhard G, Slot J, James D, Mueckler M. How Cells Absorb Glucose. Sci Am. 1992;266:86–91.

43. Tremblay F, Dubois M, Marette A. Regulation of GLUT4 traffic and function by insulin and contraction in skeletal muscle. Front Biosci a virtual Libr Med. 2003;Sep 1:d1072–84.

44. Szablewski L. Expression of glucose transporters in cancers. Biochim Biophys Acta - Rev Cancer [Internet]. Elsevier B.V.; 2013;1835:164–9. Available from: http://dx.doi.org/10.1016/j.bbcan.2012.12.004

45. Giménez-cassina A, Garcia-haro L, Choi CS, Mayowa A, Lane E, Huang H, Yildirim MA, Szlyk B, Jill K, Polak K, et al. Regulation of Hepatic Energy Metabolism and Gluconeogenesis by BAD. 2015;19:272–84.

46. Cohen G, Livovsky DM, Kapitulnik J, Sasson S. Bilirubin Increases the Expression of Glucose Transporter-1 and the Rate of Glucose Uptake in Vascular Endothelial Cells. Rev Diabet Stud [Internet]. 2006;3:127–127. Available from: http://www.soc-bdr.org/content/e4/e887/volRdsVolumes2881/issRdsIssues3801/chpRdsChapters3874/strRdsArticles3875/index_en.html?preview=preview

47. Pacák J, Točík Z, Černý M. Synthesis of 2 -Deoxy- 2 - fluoro-D-glucose. J Chem Soc D Chem Commun. 1969;77.

48. Ido T, Wan C-N, Casella V, Fowler JS, Wolf AP, Reivich M, Kuhl DE. Labeled 2-deoxy-D-

glucose analogs. 18F-labeled 2-deoxy-2-fluoro-D-glucose, 2-deoxy-2-fluoro-D-mannose and 14C-2-deoxy-2-fluoro-D-glucose. J Label Compd Radiopharm. 1978;XIV:175–83.

49. Wadsak W, Mitterhauser M. Basics and principles of radiopharmaceuticals for PET/CT. Eur J Radiol [Internet]. Elsevier Ireland Ltd; 2010;73:461–9. Available from: http://dx.doi.org/10.1016/j.ejrad.2009.12.022

50. Yu S. Review of 18F-FDG synthesis and quality control. Biomed Imaging Interv J. 2006;2.

51. Fowler JS, Ido T. Initial and subsequent approach for the synthesis of18FDG. Semin Nucl Med. 2002;32:6–12.

52. Hamacher K, Coenen HH, Stocklin G. Efficient stereospecific synthesis of no-carrier-added 2-[18F]-fluoro-2-deoxy-D-glucose using aminopolyether supported nucleophilic substitution. 1986;27:235–9.

53. Fang P, Jacobson M, Franci X, Smith R, Lowe V. Comparison of FASTlab and TRACERLAB FX synthesizers. J Nucl Med. 2007;48:325P.

54. Brown R, Leung J, Kison P, Zasadny K, Flint A, Wahl R. Glucose transporters and FDG uptake in untreated primary human non- small cell lung cancer. J Nucl Med [Internet]. 1999;40:556–65. Available from: http://ovidsp.ovid.com/ovidweb.cgi?T=JS&PAGE=reference&D=emed4&NEWS=N&AN=1999131346

55. Warburg O-H. The metabolism of tumors. New York: Richard R. Smith Inc.; 1931. 129169 p.

56. Higashi T, Tamaki N, Torizuka T, Nakamoto Y, Sakahara H, Kimura T, Honda T, Inokuma T, Katsushima S, Ohshio G. FDG Uptake, GLUT-i Glucose Transporterand Cellularity in Human Pancreatic Tumors. 1998;1727–36.

57. Bender D, Munk OL, Feng H, Keiding S. Metabolites of 18 F-FDG and 3- O - 11 C-Methylglucose in Pig Liver. 2014;

58. Southworth R, Parry CR, Parkes HG, Medina RA, Garlick PB. Tissue-specific differences in 2-fluoro-2-deoxyglucose metabolism beyond FDG-6-P: A19F NMR spectroscopy study in the rat. NMR Biomed. 2003;16:494–502.

59. Gallagher BM, Fowler JS, Gutterson NI, Macgregor RR, Wolf AP. Metabolic tical Trapping Design: as a Principle Some Factors of Radiopharmaceu Responsible for the Biodistribution Ior metabolicstudies in vivo . Metabolictrapping can be consideredas a impurity witha shorterretention. J Nucl Med. 1978;19:1154–61.

60. Mochizuki T, Tsukamoto E, Kuge Y, Kanegae K, Zhao S, Hikosaka K, Hosokawa M, Kohanawa M, Tamaki N. FDG uptake and glucose transporter subtype expressions in experimental tumor and inflammation models. J Nucl Med. 2001;42:1551–5.

61. Hulme EC, Trevethick MA. Ligand binding assays at equilibrium: Validation and interpretation. Br J Pharmacol. 2010;161:1219–37.

62. Hein P, Michel MC, Leineweber K, Wieland T, Wettschureck N OS. Receptor and Binding Studies. Practical Methods in Cardiovascular Research [Internet]. Berlin: Germany: Springer, Berlin, Heidelberg; 2005. p. 723–83. Available from: http://link.springer.com/10.1007/b137833

63. Bigott-Hennkens HM, Dannoon S, Lewis MR, Jurisson S. In vitro receptor binding assays: General methods and considerations. Q J Nucl Med Mol Imaging. 2008;52:245–53.

64. Motulsky H, Mahan L. The Kinetics of Competitive Radioligand Binding Predicted by the Law of Mass Action. Mol Pharmacol. 1984;25:1–9.

65. Yung-Chi C, Prusoff WH. Relationship between the inhibition constant (KI) and the concentration of inhibitor which causes 50 per cent inhibition (I50) of an enzymatic reaction. Biochem Pharmacol. 1973;22:3099–108.

66. Björke H, Andersson K. Measuring the affinity of a radioligand with its receptor using a rotating cell dish with in situ reference area. Appl Radiat Isot. 2006;64:32–7.

67. Zeilinger M, Pichler F, Nics L, Wadsak W, Spreitzer H, Hacker M, Mitterhauser M. New approaches for the reliable in vitro assessment of binding affinity based on high-resolution real-time data acquisition of radioligand-receptor binding kinetics. EJNMMI Res [Internet]. EJNMMI Research; 2017;7. Available from: http://dx.doi.org/10.1186/s13550-016-0249-9

68. Vraka C, Dumanic M, Racz T, Pichler F, Philippe C, Balber T, Klebermass EM, Wagner KH, Hacker M, Wadsak W, et al. A new method measuring the interaction of radiotracers

with the human P-glycoprotein (P-gp) transporter. Nucl Med Biol [Internet]. Elsevier Inc; 2018;60:29–36. Available from: https://doi.org/10.1016/j.nucmedbio.2018.02.002

69. Björke H, Andersson K. Automated, high-resolution cellular retention and uptake studies in vitro. Appl Radiat Isot. 2006;64:901–5.

70. Ridgeview Instruments AB. A typical LigandTracer measurement [Internet]. LigandTracer technology. [cited 2018 Jul 4]. Available from: http://www.ridgeviewinstruments.com/docs/LigandTracer Protocol A typical LigandTracer measurement 1.3.pdf

71. Ridgeview Instruments AB. LigandTracer technology [Internet]. LigandTracer technology. [cited 2018 Jul 4]. Available from: http://www.ridgeviewinstruments.com/docs/LigandTracer Technology Note 1.6.pdf

72. Ridgeview Instruments AB. Product specification LigandTracer Yellow [Internet]. LigandTracer technology. [cited 2018 Jul 4]. Available from: http://www.ridgeviewinstruments.com/docs/Product Specification LigandTracer Yellow 1.6.pdf

73. Yaffe D, Saxel O. Serial passaging and differentiation of myogenic cells isolated from dystrophic mouse muscle. Nature. 1977;267:192–3.

74. ATCC. Product Sheet CRL-1772 [Internet]. 2018. Available from: https://www.lgcstandards-atcc.org/products/all/CRL-1772.aspx?geo_country=at#generalinformation

75. McMahon DK, Anderson PA, Nassar R, Bunting JB, Saba Z, Oakeley AE, Malouf NN. C2C12 cells: biophysical, biochemical, and immunocytochemical properties. Am J Physiol Physiol [Internet]. 1994;266:C1795–802. Available from: http://www.physiology.org/doi/10.1152/ajpcell.1994.266.6.C1795

76. Balasubramanian R, Robaye B, Boeynaems J-M, Jacobson KA. Enhancement of Glucose Uptake in Mouse Skeletal Muscle Cells and Adipocytes by P2Y6 Receptor Agonists. PLoS One [Internet]. 2014;9:e116203. Available from: http://dx.plos.org/10.1371/journal.pone.0116203

77. ATCC. Product Sheet HB-8065 [Internet]. 2018. Available from:

https://www.lgcstandards-atcc.org/en/Products/All/HB-8065.aspx#generalinformation

78. Roe AL, Snawder JE, Benson RW, Roberts DW, Casciano DA. HepG2 cells: an in vitro model for P450-dependent metabolism of acetaminophen. 1993.

79. Xia J. Flavonoids as potential anti-hepatocellular carcinoma agents: Recent approaches using HepG2 cell line. Drug Discov Ther [Internet]. 2013;7:1–8. Available from: http://www.ddtjournal.com/getabstract.php?id=642

80. Dehn P, White C, Conners D, SHIPKEY G, CUMBO TA. Characterization of the human hepatocellular carcinoma (hepg2) cell line as an in vitro model for cadmium toxicity studies. Vitr Cell Dev Biol [Internet]. 2004;40:172–82. Available from: http://link.springer.com/article/10.1290/1543-706X(2004)40%3C172:COTHHC%3E2.0.CO;2%5Cnhttp://link.springer.com/article/10.1290/1543-706X(2004)40%3C172:COTHHC%3E2.0.CO;2#page-1%5Cnhttp://link.springer.com/content/pdf/10.1290/1543-706X(2004)

81. Galvao J, Davis B, Tilley M, Normando E, Duchen MR, Cordeiro MF. Unexpected low-dose toxicity of the universal solvent DMSO. FASEB J. 2014;28:1317–30.

82. Molnar P, Wang W, Natarajan A, Rumsey JW, Hickman JJ. Photolithographic Patterning of C2C12 Myotubes using Vitronectin as Growth Substrate in Serum-Free Medium. Biotechnol Prog. 2007;23:265–268.

83. Vítek L. Bilirubin and atherosclerotic diseases. Physiol Res [Internet]. 2017;66:S11–20. Available from: www.biomed.cas.cz/physiolres%0Ahttp://www.ncbi.nlm.nih.gov/pubmed/28379026

84. Liu J, Dong H, Zhang Y, Cao M, Song L, Pan Q, Bulmer A, Adams DB, Dong X, Wang H. Bilirubin increases insulin sensitivity by regulating cholesterol metabolism, adipokines and PPAR 3 Levels. Sci Rep [Internet]. Nature Publishing Group; 2015;5:1–12. Available from: http://dx.doi.org/10.1038/srep09886

85. Dong H, Huang H, Yun X, Kim DS, Yue Y, Wu H, Sutter A, Chavin KD, Otterbein LE, Adams DB, et al. Bilirubin increases insulin sensitivity in leptin-receptor deficient and diet-induced obese mice through suppression of ER stress and chronic inflammation.

Endocrinology. 2014;155:818–28.

86. Troughton JA, Woodside J V., Young IS, Arveiler D, Amouyel P, Ferrières J, Ducimetière P, Patterson CC, Kee F, Yarnell JWG, et al. Bilirubin and coronary heart disease risk in the Prospective Epidemiological Study of Myocardial Infarction (PRIME). Eur J Cardiovasc Prev Rehabil [Internet]. 2007;14:79–84. Available from: http://journals.sagepub.com/doi/10.1097/01.hjr.0000230097.81202.9f

87. He M, Nitti M, Piras S, Furfaro AL, Traverso N, Pronzato MA, Mann GE. Heme oxygenase-1-derived bilirubin protects endothelial cells against high glucose-induced damage. Free Radic Biol Med [Internet]. Elsevier; 2015;89:91–8. Available from: http://dx.doi.org/10.1016/j.freeradbiomed.2015.07.151

88. Clark JE, Foresti R, Green CJ, Motterlini R. Dynamics of haem oxygenase-1 expression and bilirubin production in cellular protection against oxidative stress. Biochem J. 2000;348 Pt 3:615–9.

89. Peyton KJ, Shebib AR, Azam MA, Liu X, Tulis DA, Durante W. Bilirubin Inhibits Neointima Formation and Vascular Smooth Muscle Cell Proliferation and Migration. Front Pharmacol [Internet]. 2012;3:1–8. Available from: http://journal.frontiersin.org/article/10.3389/fphar.2012.00048/abstract

90. Cooper GM, Hausman RE. Cell-Cell Interactions. The Cell: A Molecular Approach [Internet]. 2nd editio. Sunderland, MA: Sinauer Associates; 2000. Available from: https://www.ncbi.nlm.nih.gov/books/NBK9851/